Dynamic Modeling of the Central Carbon Metabolism of *Escherichia coli*

Christophe Chassagnole, Naruemol Noisommit-Rizzi, Joachim W. Schmid, Klaus Mauch, Matthias Reuss

Institute of Biochemical Engineering, University of Stuttgart, Allmandring 31, D-70569 Stuttgart, Germany; telephone: +49-0-711-685-7532; fax +49-0-711-685-5164; e-mail: reuss@ibvt.uni-stuttgart.de

Abstract: Application of metabolic engineering principles to the rational design of microbial production processes crucially depends on the ability to describe quantitatively the systemic behavior of the central carbon metabolism to redirect carbon fluxes to the product-forming pathways. Despite the importance for several production processes, development of an essential dynamic model for central carbon metabolism of *Escherichia coli* has been severely hampered by the current lack of kinetic information on the dynamics of the metabolic reactions. Here we present the design and experimental validation of such a dynamic model, which, for the first time, links the sugar transport system (i.e., phosphotransferase system [PTS]) with the reactions of glycolysis and the pentose-phosphate pathway. Experimental observations of intracellular concentrations of metabolites and cometabolites at transient conditions are used to validate the structure of the model and to estimate the kinetic parameters. Further analysis of the detailed characteristics of the system offers the possibility of studying important questions regarding the stability and control of metabolic fluxes. © 2002 Wiley Periodicals, Inc. *Biotechnol Bioeng* **79**: 53–73; 2002.

Keywords: dynamic model; *Escherichia coli*; intracellular metabolites; transient conditions; control and stability analysis

INTRODUCTION

One of the most ambitious and challenging goals of metabolic engineering is the design of biological systems based on quantitative predictions with the aid of mathematical models. Whereas the potential and promise of biological systems modeling is substantial, several obstacles are still encountered when addressing the aforementioned issue of quantitative design. This is particularly because of the well-known difficulties in assessing enzyme kinetics under in vivo conditions as a prerequisite for a sound quantitative analysis of the reaction pathways. Indeed, success in the development of rigorous dynamic models for metabolic systems has been severely hampered by the current lack of kinetic information on the dynamics of the reactions (Edwards and Palsson, 2000).

Because the many biochemical details of the metabolic networks appear overwhelming at first sight, there is a demand for decreasing the enormous complexity of the problem. Concepts generated toward this end must be examined in the context of the intended purpose of the model. When focusing on objectives of flux amplification for increase of specific productivities in the industrial manufacturing of metabolites, the task is most often specifically reduced to an amplification of the central metabolic pathways (Stephanopoulos and Simpson, 1997). Of course, modeling of the many interconnected reactions of the main supply route to product-forming pathways remains a demanding undertaking, but the model of the system required for identification of targets for manipulation shows a manageable dimension.

The range of validity is another important issue for purposes of generating the model. If dynamic models are based on measurement of intracellular responses to external disturbances, many of the effects observed can be attributed to cellular functions beyond the intended application. Thus, if the focus is on prediction of the modulation of enzyme concentrations, sophisticated phenomena, such as stress response or the dynamics of transcription and translation processes caused by the disturbance, are less important. To circumvent the superposition of these side effects, the time scale of the experimental observation used for model identification should be as brief as possible.

Establishing kinetic models of cellular metabolism is always embedded within the dispute if, according to the traditional biochemistry point of view, models can be designed by an aggregation of in vitro enzyme kinetics or, alternatively, in vivo measurements of metabolites should be applied for identification of kinetic properties. There are two pivotal questions regarding the applica-

tion of in vitro kinetics for studying metabolic networks: (1) To what extent does the multitude of interacting processes inside the cell lead to a kinetic behavior that differs from in vitro conditions? (2) What is the influence of the functioning of the entire ensemble? (Or, can we simply sum up every enzyme reaction to understand the system quantitatively?). By comparison of in vitro, in situ, and in vivo results for enzyme kinetics of the phosphofructokinase I system in *Saccharomyces cerevisiae*, it has been demonstrated that remarkable differences in structure of the kinetic expressions, as well as in parameter values, can be observed in the case of such complex enzyme systems (Mauch et al., 2000). Consequently, we recommend using the measurements of intracellular metabolites for identification of in vivo enzyme kinetics in a similar way as measurements are applied to identification of in vitro kinetics within test tubes. The main difference is the dimension of the parameter space.

The aforementioned strategies provide a means for designing dynamic pathway models. However, it is clear that, faced with the many open questions, the "degree of truth" or theoretically justifiable background remains limited. As such, it is necessary to identify the dynamic determinants (Palsson, 2000; Stephanopoulos and Simpson, 1997). These determinants are related to essential structural properties of the model and are relatively insensitive to the exact numerical value of the kinetic parameters. Modeling of the central metabolism of *Escherichia coli* as illustrated in this study results in an impressive example in support of this hypothesis. The strong influence of feedforward and feedback regulations manifests itself in a dynamic pattern of metabolites clearly pointing to such structural determinants, which cannot be compensated by parameter fitting. As a consequence of this rigid structure, the targeted design for flux amplification must rest on a framework of coordinated structural changes of the network instead of amplification of single enzymes (Sauer et al., 1999).

The objective of this study is to model the kinetic behavior of the central carbon metabolism of *Escherichia coli*. The necessity of obtaining a quantitative understanding of the pathways responsible for the production of precursors for biosynthetic pathways has been demonstrated for the production of aromatic compounds by several research groups (Berry, 1996; Flores et al., 1996; Gosset et al., 1996; Liao et al., 1996; Patnaik and Liao, 1994; Patnaik et al., 1995; Lu and Liao, 1997; Stephanopoulos and Simpson, 1997; Stephanolopoulos et al., 1998). Despite the importance of the central carbon route, none of these contributions have assessed a kinetic model of the key pathways of *Escherichia coli*. Stephanopoulos and Simpson (1997) applied the model for the glycolysis of *Saccharomyces cerevisiae* as suggested by Galazzo and Bailey (1990, 1991). Torres (1997) used the model for erythrocytes developed by Schuster and Holzhütter (1995). It is the

strength of the structural determinant of the phosphotransferase system (PTS) (Gosset et al., 1996; Liao et al., 1996; Patnaik and Liao, 1994) that has been neglected in these approaches.

The design of the dynamic model of the central carbon route in *Escherichia coli* (PTS system, glycolysis, pentosephosphate pathway, and storage material) presented herein rests on dynamic measurements of metabolites in a manner similar to that of *Saccharomyces cerevisiae* under aerobic (Rizzi et al., 1997; Theobald et al., 1997; Vaseghi et al., 1999) and anaerobic (Mauch et al., 2001) growth conditions. The dynamic responses of intracellular metabolites to a pulse of glucose were measured in continuous culture employing a new automatic stopped-flow sampling device (Buziol et al., 2000, 2001) as well as a manual sampling technique (Theobald et al., 1993, 1997). These measurements permit analysis of transient behavior at the second and subsecond time scale.

The mathematical model provides a means for rigorous application of dynamic stability analysis and metabolic control analysis (MCA) to obtain a first insight into the possible targets for the envisaged redesign of central carbon metabolism.

MATERIALS AND METHODS

Organism and Growth Conditions

Escherichia coli K-12 strain W3110, obtained from the Genetic Stock Center, Yale University (New Haven, CT), was grown at under glucose limitation at 35°C in a stirred-tank bioreactor (KLF 2000, Bioengineering, Wald, Switzerland), with a working volume of 1.5 L. The airflow was kept at 1 vvm and the pH was controlled at 7.0 by addition of 2 M NaOH. To prevent foam formation, small quantities (1 mL) of Contraspum 210 (Zschimmer & Schwarz, Lahnstein, Germany) were added periodically. The concentrations of components in the synthetic mineral medium were precalculated from elementary balancing for production of 10 g dry weight (DW) per liter: 4.0 g/L Na_2SO_4; 5.36 g/L $(NH_4)_2SO_4$; 1.0 g/L NH_4Cl, 7.3 g/L K_2HPO_4; 1.8 g/L NaH_2PO_4 H_2O; 120 g/L $(NH_4)_2$-H-citrate; 4.0 mL/L $MgSO_4$ (1 M); 6.0 ml/L trace element solution; 0.02 g/L thiamine; and 20.0 g/L glucose. The bioreactor was connected to an exhaust air analysis device consisting of a paramagnetic oxygen analyzer (Oxygor 6N) and an infrared CO_2 analyzer (Unor 6N), both from Maihak (Hamburg, Germany).

Glucose Pulse Experiments

Starting from steady-state conditions at $D = 0.1 \pm 0.002$ h^{-1}, for which the glucose concentration was $C_{glc}^{extracellular} = 12 \pm 1.5$ mg/L, a pulse of glucose (3 mL sterilized solution [15% w/w]) was injected with a syringe

at time $t = t_0$ to give an initial bulk concentration of 0.3 g/L. The volume injected was <1% of the total working volume, and therefore its influence on dilution rate was neglected.

After injection of the glucose, samples were taken manually every 3 s with vacuum-sealed, precooled glass tubes containing the quenching/extraction solution as described by Theobald et al. (1993, 1997).

For measurements of the intracellular response in the time period of <1 s after the stimulus of extracellular glucose the stopped-flow sampling technique (Buziol et al., 2000, 2001) was applied. In this sampling procedure, a continuous stream of biosuspension leaving the bioreactor was mixed with a glucose solution in a turbulent mixing chamber and samples taken with the aid of a cascade of three-way valves and sampling tubes containing the quenching fluid. The residence time in the plug flow then corresponded to the different reaction times.

Quenching and Extraction

The different quenching and extraction procedures are summarized in Figure 1. The treatment of the samples for measurement of extracellular concentrations of glucose and acetate is the same as described by Theobald et al. (1993, 1997). For measurements of acid-labile metabolites, such as G6P, F6P, PEP, Pyr, and 6PG, the biosuspension was quenched with liquid nitrogen (−196°C). The sample was kept for 10 min at −25°C. After evaporation of the liquid nitrogen and weighing of the sample, extraction was performed by adding a 0.5 sample volume of Tris-H$_2$SO$_4$/ethylene-diamine tetra-acetic acid (EDTA) (pH 7.75). After 1 min, the sample was thawed and pipetted into another 0.5 sample volume of Tris-H$_2$SO$_4$/EDTA at 90°C. The mixture was then thoroughly vortexed, centrifuged after 10 min (16,000g, 1°C, 15 min), and finally filtered (pore size 0.2 μm).

GAP, FDP, adenine nucleotides (AMP, ADP, and ATP), NAD$^+$, and NADP$^+$ are acid-stable metabolites and can be quenched and extracted with perchloric acid solutions (35% [w/w], −25°C) as described by Theobald et al. (1993, 1997).

For measurement of NAD(P)H, the sample was incubated at −25°C with 0.3N KOH after quenching in liquid nitrogen. The extract was thawed at 1°C for 30 min. After incubation at 60°C for 7 min, the extract was cooled to 0°C. Before analysis, the extract was neutralized to pH 7 with 0.3N HCl. The neutralized extract was kept for at least 10 min to precipitate proteins before centrifuging at 16,000g for 15 min and filtering (pore size 0.2 μm).

Analytical Methods

The concentrations of the extracellular metabolites (glucose, acetate) and most of the intracellular metabolites were determined as described previously (Theobald et al., 1997). Improved analysis of the adenine nucleotides was summarized by Mailinger et al. (1998) and Meyer et al. (1999). The metabolites and cometabolites from the pentose-phosphate pathway (6PG, NADP$^+$, and NADPH) were measured according to Vaseghi et al. (1999).

MODELING

Model Structure

The dynamic model of the Embden–Meyerhof–Parnas pathway and pentose-phosphate pathway of *Escherichia coli* consists of mass balance equations for extracellular glucose and for the intracellular metabolites as shown in Figure 2. These mass balances take the following form:

$$\frac{dC_i}{dt} = \sum_j \nu_{ij} r_j - \mu C_i \qquad (1)$$

where C_i denotes the concentration of metabolite i, μ is the specific growth rate, and ν_{ij} is the stoichiometric coefficient for this metabolite in reaction j, the rate of which is r_j. The balance equation for extracellular glucose is expressed as:

$$\frac{dC_{\text{glc}}^{\text{extracellular}}}{dt} = D(C_{\text{glc}}^{\text{feed}} - C_{\text{glc}}^{\text{extracellular}}) + f_{\text{pulse}} - \frac{C_{\text{x}} r_{\text{PTS}}}{\rho_{\text{x}}} \qquad (2)$$

where $C_{\text{glc}}^{\text{feed}}$ is the glucose concentration in the feed, $C_{\text{glc}}^{\text{extracellular}}$ is the extracellular glucose concentration, C_{x} is the biomass concentration, and ρ_{x} is the specific weight of the biomass. The term f_{pulse} provides allowance for the sudden change of glucose concentration caused by the glucose pulse. Figure 2 outlines the metabolic details of the model, and Table I lists the complete set of balance equations.
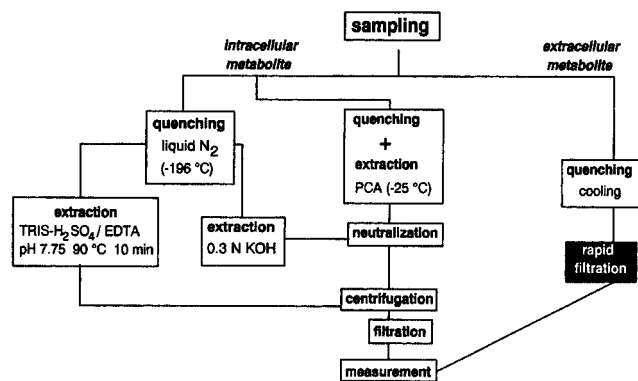

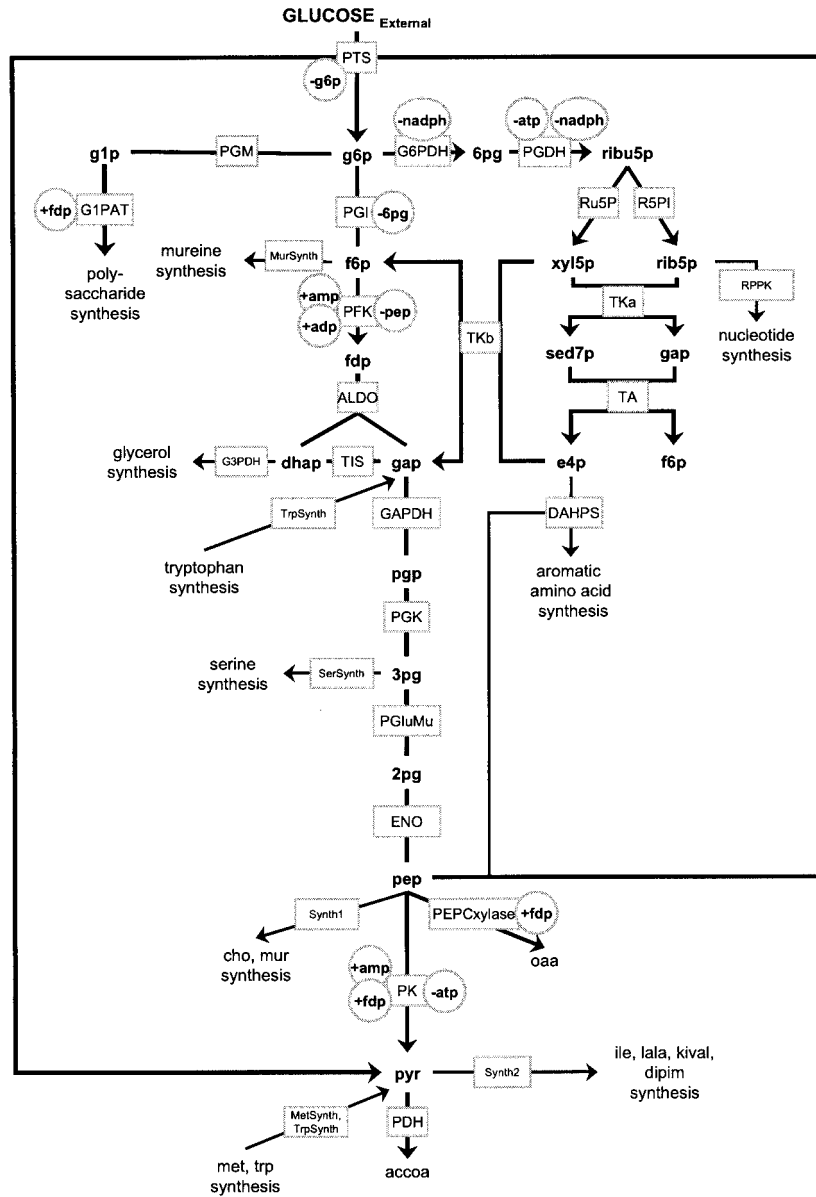**Figure 1.** Sampling technique and procedure.

Figure 2. Structure of the metabolic model of glycolysis and ppp in *E. coli*. Squares: enzyme activities; circles: regulatory effects.

Estimation of Maximum Reaction Rates

The rate of the enzyme i at steady state is given by:

$$\tilde{r}_i = r_i^{\max} f_i(\tilde{C}_i, \tilde{P}_i) \tag{3}$$

where $\tilde{P}_i$ is the parameter vector and $\tilde{C}_i$ is the steady-state concentration vector of the metabolites involved in the reaction. From the previous equation, the maximal rate was calculated (Rizzi et al., 1997):

$$r_i^{\max} = \frac{\tilde{r}_i}{f_i(\tilde{C}_i, \tilde{P}_i)} \tag{4}$$

The dynamic model represents a subsystem of a larger stationary model which was used to observe the intracellular fluxes $\tilde{r}_i$ in Eq. (4) at defined physiological conditions. In contrast to the dynamic subsystem, the stationary model allows the integrated usage of experimentally derived uptake and excretion rates (cf. Table II) taken from measurements under the same conditions from which the glucose pulse experiments were started. The Appendix shows the complete set of equations considered in the flux analysis.

If present, the stoichiometry of these reactions was taken from the internet database, ECOCYC (Karp et al., 1999), or from Neidhardt et al. (1996).

Uncertainties concerning the flux distribution were related to some of the reactions in which NAD/(NADH + H$^+$) and NADP/(NADPH + H$^+$) are involved. The predictions of the flux distribution shown in Figure 3 rest upon the assumption that NAD$^+$ is the coenzyme

Table I. Mass balance equations.

$$\frac{dC_{glc}^{extracellular}}{dt} = D\left(C_{glc}^{feed} - C_{glc}^{extracellular}\right) + f_{pulse} - \frac{C_x r_{PTS}}{\rho_x}$$

$$\frac{dC_{g6p}}{dt} = r_{PTS} - r_{PGI} - r_{G6PDH} - r_{PGM} - \mu C_{g6p}$$

$$\frac{dC_{f6p}}{dt} = r_{PGI} - r_{PFK} + r_{TKb} + r_{TA} - 2r_{MurSynth} - \mu C_{f6p}$$

$$\frac{dC_{fdp}}{dt} = r_{PFK} - r_{ALDO} - \mu C_{fdp}$$

$$\frac{dC_{gap}}{dt} = r_{ALDO} + r_{TIS} - r_{GAPDH} + r_{TKa} + r_{TKb} - r_{TA} + r_{TrpSynth} - \mu C_{gap}$$

$$\frac{dC_{dhap}}{dt} = r_{ALDO} - r_{TIS} - r_{G3PDH} - \mu C_{dhap}$$

$$\frac{dC_{pgp}}{dt} = r_{GAPDH} - r_{PGK} - \mu C_{pgp}$$

$$\frac{dC_{3pg}}{dt} = r_{PGK} - r_{PGluMu} - r_{SerSynth} - \mu C_{3pg}$$

$$\frac{dC_{2pg}}{dt} = r_{PGluMu} - r_{ENO} - \mu C_{2pg}$$

$$\frac{dC_{pep}}{dt} = r_{ENO} - r_{PK} - r_{PTS} - r_{PEPCxylase} - r_{DAHPS} - r_{Synth1}^a - \mu C_{pep}$$

$$\frac{dC_{pyr}}{dt} = r_{PK} + r_{PTS} - r_{PDH} - r_{Synth2}^b + r_{MetSynth} + r_{TrpSynth} - \mu C_{pyr}$$

$$\frac{dC_{6pg}}{dt} = r_{G6PDH} - r_{PGDH} - \mu C_{6pg}$$

$$\frac{dC_{ribu5p}}{dt} = r_{PGDH} - r_{Ru5P} - r_{R5PI} - \mu C_{ribu5p}$$

$$\frac{dC_{xyl5p}}{dt} = r_{Ru5P} - r_{TKa} - r_{TKb} - \mu C_{xyl5p}$$

$$\frac{dC_{sed7p}}{dt} = r_{TKa} - r_{TA} - \mu C_{sed7p}$$

$$\frac{dC_{rib5p}}{dt} = r_{R5PI} - r_{TKa} - r_{RPPK} - \mu C_{rib5p}$$

$$\frac{dC_{e4p}}{dt} = r_{TA} - r_{TKb} - r_{DAHPS} - \mu C_{e4p}$$

$$\frac{dC_{g1p}}{dt} = r_{PGM} - r_{G1PAT} - \mu C_{g1p}$$

[a] $r_{Synth1} = r_{ChoSynth} + r_{MurSynth}$.
[b] $r_{Synth2} = r_{IleSynth} + r_{AlaSynth} + r_{KivalSynth} + r_{DipimSynth}$.

of isocitrate dehydrogenase. Despite the fact that this assumption has been applied in many network models for *Escherichia coli* (see, e.g., Pramanik and Keasling, 1997; Varner, 2000), we also studied the influence of the alternative of $NADP^+$ as a cofactor of this reaction. As expected, the predicted fluxes showed a pronounced change in the ratio of fluxes through glycolysis and the pentose-phosphate pathway. However, it is of interest to note that the difference in the predicted ratio of fluxes showed no significant effect on the identified kinetic structure of rate expressions and kinetic parameters of the dynamic model. More investigations, particularly inclusion of measured flux distributions, are needed to draw further conclusions regarding the relation between steady-state fluxes and dynamic properties of the system.

Table II. Estimated biomass composition of *Escherichia coli* and measured uptake and excretion fluxes in a continuous culture, both at a growth rate of $\mu = 0.1 \pm 0.002$ h^{-1}.

Compound	Proportion [% g/g DW]	Source
Protein	72	[a]
DNA	4	
RNA	10	
Lipids	9	[b]
Polysaccharides	2.5	
Mureine	2.5	

Amino acids[c]		Nucleotides[b]		Lipid monomers[b]		Fatty acids[c]	
Proportion [% Amount]		Proportion [% Amount]		Proportion [% Amount]		Proportion [% Amount]	
Ala	11.4	amp	26.2	Glycerol	8.3	*Saturated:*	
Arg	5.0	gmp	32.2	Ethanolamine	25.1	C10	0.08
Asp	5.0	ump	21.6	Fatty acids	66.7	C12	3.53
Asn	5.0	cmp	20.0			C13	0.27
Cys	1.7	damp	24.6			C14	12.84
Glu	5.6	dgmp	25.4			C15	8.00
Gln	5.6	dtmp	24.6			C16	40.64
Gly	8.6	dcmp	25.4			C17	20.09
His	1.7					C18	1.03
Ile	4.6					C19	0.59
Leu	9.1						
Lys	5.6					*Unsaturated:*	
Met	2.4					C13	0.08
Phe	3.4					C14	0.36
Pro	4.2					C15	0.16
Ser	4.9					C16	9.72
Thr	5.3					C17	0.19
Trp	1.1					C18	2.48
Tyr	2.8						
Val	7.2						

Glucose uptake	9.2 ± 0.9 mmol L^{-1} h^{-1}
Acetate excretion	Not detectable
Oxygen uptake	24.3 ± 2.4 mmol L^{-1} h^{-1}
Carbon dioxide excretion	24.8 ± 2.5 mmol L^{-1} h^{-1}

[a]Ingraham et al. (1983); [b]Neidhardt et al. (1996); [c]Pramanik and Keasling (1998).

Macromolecular composition of biomass was estimated according to Ingraham et al. (1983), Neidhardt et al. (1996), and Pramanik and Keasling (1998). These data are shown in Table II.

For the resulting linear equation system, the degrees of freedom = 3. The set of equations was solved analytically based on steady-state measurements of a continuous culture at a growth rate of $\mu = 0.1 \pm 0.002$ h^{-1} (experimentally derived uptake and excretion rates; cf. Table II). Extracellular acetate was not detected, thus the system was overdetermined by one. Using the standard deviations given in Table II, an error criterium of $h_\varepsilon = 0.017 < \chi^2 = 3.8$ was obtained, indicating no inconsistency.

The resulting steady-state fluxes for the reactions included in the dynamic model are shown in Figure 3.

Kinetic Rate Expressions

The kinetic equations for the various enzyme-catalyzed reactions are shown in Table IV. The kinetics are based on published information obtained from in vitro investigations with the purified enzymes. For cases in which the experimental observations did not permit enough sensitivity, complex mechanisms were reduced to empirical rate expressions.

Glucose Transport System

Experimental evidence has shown that sugar transport at glucose-limited growth conditions is characterized by the presence of multiple transport systems (Ferenci, 1996). Despite this complex situation only the PTS has been taken into account. The rate expression for the PTS [Eq. (9)] was brought forth by Liao et al. (1996). The potential control of the PEP:Pyr ratio can be predicted by a model that assumes equilibrium of the reaction involving enzyme I, HPr, and IIA^{Glc} (Liao et al., 1996) within the PTS and the rate-limiting step to be the final step of glucose transport and phosphorylation. According to Kaback (1969) and Clark and Holms (1976), the PTS is
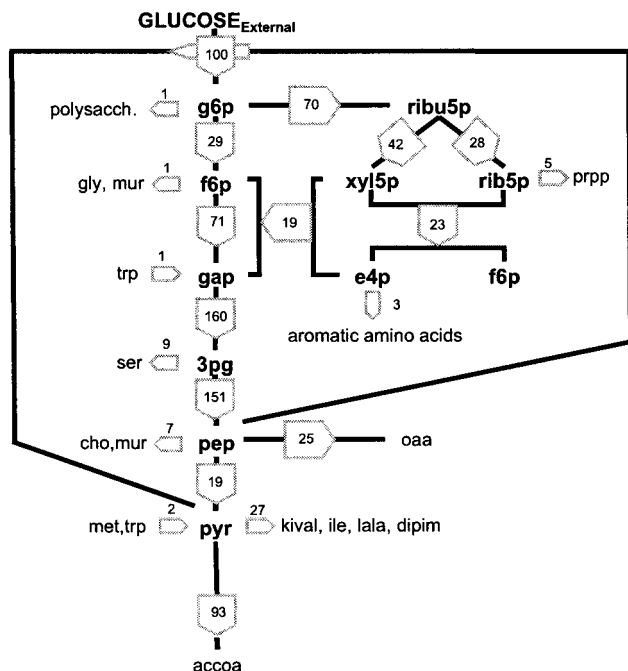
Figure 3. Steady-state flux distribution of glycolysis and ppp for a dilution rate of $D = 0.1 \ h^{-1}$.

inhibited by glucose-6-phosphate. The rate expression shown in Table IV accounts for this inhibition.

Glycolysis

Literature references and specific comments regarding the kinetics chosen for the individual reactions are summarized in Table III. The corresponding rate expressions are shown in Table IV. A few brief explanations are in order concerning the selection of some of the kinetics.

The two glucose-6-phosphate isomerase (PGI) isoenzymes reported for *E. coli* (Schreyer and Bock, 1980) have been lumped into one rate expression [Eq. (10)] as the kinetic properties of the two forms are considered to be identical (Schreyer and Bock, 1980).

Two forms of phosphofructokinase (PFK) are present in *E. coli* (Karp et al., 1999) for which PFK-1 is the predominant form, accounting for 90% of the total activity (Karp et al., 1999). Thus, only this form was considered in the model. Inhibition by phosphoenolpyruvate as described for *E. coli* by Kotlarz et al. (1975) has been included.

The pyruvate kinase reaction is catalyzed by two isoenzymes (PKI and PKII) as well. PKI is activated by fructose-1,6-bisphosphate (FDP) and inhibited by ATP, whereas AMP activates PKII. Because the individual activities of the two isoforms cannot be distinguished from steady-state metabolic flux analysis, the kinetics of the two enzymes were lumped into one equation. The resulting rate expression [Eq. (10)] represents a combination of the aforementioned regulation of the two

isoenzymes. The equation is based on the kinetics suggested by Johannes and Hess (1973), with an additional term for AMP activation.

Biosynthetic and Anaplerotic Reactions

Consumption of phosphoenolpyruvate (PEP) for mureine and chorismate synthesis has been expressed as simple Michaelis–Menten kinetics [Synthesis 1, Eq. (37)]. The same approach holds for the consumption of pyruvate for synthesis of isoleucine, alanine, α-ketoisovalerate, and diaminopimelate [Synthesis 2, Eq. (38)].

Pentose-Phosphate Pathway (ppp)

The model for this part of the metabolism is equivalent to the approach suggested for *Saccharomyces cerevisiae* by Vaseghi et al. (1999). According to Sanwal (1970), G6PDH is inhibited only by NADPH. The ATP inhibition observed for G6PDH in yeast has not been found in *E. coli*. For PGDH, however, inhibition by NADPH and ATP is similar to what has been observed for the yeast enzyme (Orozco, 1979).

The reactions of the nonoxidative part of the ppp were expressed by reversible mass action kinetics [Eqs. (32)–(36)].

It must be emphasized that, in the complete model, the cometabolites (nad, nadh, nadp, nadph, amp, adp, and atp) remain unbalanced (for analytical functions, see Table VI and Fig. 4).

Steady-State Concentrations

Steady-state concentrations are required for the estimation of the maximal rates, v_{max} [Eq. (4)], and as initial conditions for the integration of the dynamic model. Some of these concentrations are available from the measurements of intracellular metabolites. The remaining concentrations are estimated from a near-equilibrium assumption for the reaction of interest. The near-equilibrium constant was initially introduced by Schauer et al. (1981) and applied to the estimation of steady-state concentrations in the ppp by Vaseghi et al. (1999). The near-equilibrium constant for the *j*th reaction, K_j, is given by:

$$K_j = \delta_j K_{eq,j} = \delta_j \prod_i \tilde{C}_i^{\nu_{i,j}} \tag{5}$$

where:

$$0 \leq \delta_j \leq 1 \tag{6}$$

where $K_{eq,j}$ is the equilibrium constant of the *j*th reaction, $\tilde{C}_i$ is the steady-state concentration of the compound *i*, and $\nu_{i,j}$ is the stoichiometric coefficient of compound *i* in reaction *j*.

Table III. Kinetic types and regulations of the different enzymatic reactions.

Enzymatic reaction	Kinetic type description	Activation	Inhibition	Equation number
PTS	Cf. Text		g6p[a,b]	(9)
PGI	Reversible Michaelis–Menten[c]		6pg[d]	(10)
PFK	Allosteric enzyme[e]	amp, adp[e]	pep[f]	(11)
Aldo	Ordered uni-bi mechanism[c]			(12)
TIS	Reversible Michaelis–Menten[c]			(13)
GAPDH, PGK	Two-substrate reversible Michaelis–Menten			(14), (15)
PGluMu, ENO	Reversible Michaelis–Menten			(16), (17)
PK	Allosteric regulation[g]	fdp[g], amp	atp[g]	(18)
PDH	Hill equation			(19)
PEPCxylase	Two-substrate equation with allosteric activation	fdp[h,i]		(20)
PGM	Reversible Michaelis–Menten			(21)
G1PAT	Allosteric activation	fdp[j]		(22)
Mureine synthesis, tryptophan synthesis, methionine synthesis	Constant level corresponding to the steady state flux			(26), (28), (29)
RPPK, G3PDH, serine synthesis	Michaelis–Menten			(23), (24), (25)
Synthesis 1 and 2	Michaelis–Menten			(37), (38)
DAHPS	Hill equation[k]			(27)
G6PDH	Two-substrate irreversible Michaelis–Menten[l]		nadph[m]	(30)
PGDH	Two-substrate irreversible Michaelis–Menten[l]		nadph, atp[n]	(31)
Ru5P, R5PI, TKa, TKb, and TA	Reversible mass action kinetic			(32), (33), (34), (35), (36)

[a]Kaback (1969); [b]Clark and Holms (1976); [c]Richter et al. (1975); [d]Schreyer and Bock (1980); [e]Hofmann and Kopperschläger (1982); [f]Kotlarz et al. (1975); [g]Johannes and Hess (1973); [h]Kameshita et al. (1979); [i]Yoshinaga (1977); [j]Preiss et al. (1975); [k]Akowski and Bauerle (1970); [l]Vaseghi et al. (1999); [m]Sanwal (l970); [n]Orozco de Silva (1979).

For a first estimation of the steady-state concentrations, a deviation of 10% from thermodynamic equilibrium is assumed. Thus, δ_j is set to 0.9 for all near-equilibrium reactions.

For estimation of the concentrations of 1,3-bisphosphoglycerate (pgp), 3-phosphoglycerate (3pg) and 2-phosphoglycerate (2pg), measured values of ATP, ADP, and phosphoenolpyruvate (pep) were applied along with equilibrium constants for the reactions catalyzed by 3-phosphoglycerate kinase (PGK) (Ni and Savageau, 1996), phosphoglycerate mutase, and enolase (Bakker et al., 1997). The ratio of the estimated concentrations of pep and 3pg shows reasonable agreement to measured values of Schaefer et al. (1999) and Bhattacharya et al. (1995) for *E. coli*. A similar ratio was also found by Bakker et al. (1997) in *Trypanosoma brucei* and by Mulquiney and Kuchel (1999) in human erythrocytes.

A serious discrepancy between the results from application of the near-equilibrium concept and measured concentrations was detected in the reactions catalyzed by triosephosphate isomerase (TIS) and aldolase (Aldo). The two estimated values for the concentrations of DHAP from measured GAP and FDP concentrations together with published data for the equilibrium constants defined by:

$$K_{\text{TIS},eq} = C_{\text{GAP}}/C_{\text{DHAP}} \tag{7}$$

and:

$$K_{\text{Aldo},eq} = (C_{\text{GAP}} \cdot C_{\text{DHAP}})/C_{\text{FDP}} \tag{8}$$

resulted in an order of magnitude difference. This disagreement indicates that one and/or the other assumption regarding near equilibrium was not adequate. A similar inconsistency with respect to the equilibrium assumption of the two reactions was observed by Schaefer et al. (1999). Without attempting a detailed study of these phenomena we chose to employ the ratio $C_{\text{GAP}}/C_{\text{DHAP}} = 3/2.3$, as measured by Schaefer et al. (1999).

Near-equilibrium conditions were assumed for the five reactions of the nonoxidative part of the pentose-phosphate pathway (Ru5P, R5PI, TKa, TKb, and TA) (Vaseghi et al., 1999). The metabolite concentrations of ribu5p, rib5p, xyl5p, sed7p, and e4p were estimated from measured steady-state concentrations of f6p and gap.

Estimated and measured steady-state concentrations are listed in Table V.

Table IV. Kinetic rate equations.

Phosphotransferase system:

$$r_{\text{PTS}} = \frac{r_{\text{PTS}}^{\max} C_{\text{glc}}^{\text{extracellular}} \frac{C_{\text{pep}}}{C_{\text{pyr}}}}{\left(K_{\text{PTS},a1} + K_{\text{PTS},a2}\frac{C_{\text{pep}}}{C_{\text{pyr}}} + K_{\text{PTS},a3}C_{\text{glc}}^{\text{extracellular}} + C_{\text{glc}}^{\text{extracellular}}\frac{C_{\text{pep}}}{C_{\text{pyr}}}\right)\left(1 + \frac{C_{\text{g6p}}^{n_{PTS,g6p}}}{K_{\text{PTS},g6p}}\right)} \tag{9}$$

Phosphoglucoisomerase:

$$r_{\text{PGI}} = \frac{r_{\text{PGI}}^{\max}\left(C_{\text{g6p}} - \frac{C_{\text{f6p}}}{K_{\text{PGI,eq}}}\right)}{K_{\text{PGI,g6p}}\left(1 + \frac{C_{\text{f6p}}}{K_{\text{PGI,f6p}}\left(1+\frac{C_{\text{6pg}}}{K_{\text{PGI,f6p,6pginh}}}\right)} + \frac{C_{\text{6pg}}}{K_{\text{PGI,g6p,6pginh}}}\right) + C_{\text{g6p}}} \tag{10}$$

Phosphofructokinase:

$$r_{\text{PFK}} = \frac{r_{\text{PFK}}^{\max} C_{\text{atp}} C_{\text{f6p}}}{\left(C_{\text{atp}} + K_{\text{PFK,atp,s}}\left(1 + \frac{C_{\text{adp}}}{K_{\text{PFK,adp,c}}}\right)\right)\left(C_{\text{f6p}} + K_{\text{PFK,f6p,s}}\frac{A}{B}\right)\left(1 + \frac{L_{\text{PFK}}}{\left(1+C_{\text{f6p}}\frac{B}{K_{\text{PFK,f6p,s}}A}\right)^{n_{\text{PFK}}}}\right)} \tag{11}$$

$$A = 1 + \frac{C_{\text{pep}}}{K_{\text{PFK,pep}}} + \frac{C_{\text{adp}}}{K_{\text{PFK,adp,b}}} + \frac{C_{\text{amp}}}{K_{\text{PFK,amp,b}}}$$

$$B = 1 + \frac{C_{\text{adp}}}{K_{\text{PFK,adp,a}}} + \frac{C_{\text{amp}}}{K_{\text{PFK,amp,a}}}$$

Aldolase:

$$r_{\text{ALDO}} = \frac{r_{\text{ALDO}}^{\max}\left(C_{\text{fdp}} - \frac{C_{\text{gap}}C_{\text{dhap}}}{K_{\text{ALDO,eq}}}\right)}{K_{\text{ALDO,fdp}} + C_{\text{fdp}} + \frac{K_{\text{ALDO,gap}}C_{\text{dhap}}}{K_{\text{ALDO,eq}}V_{\text{ALDO,blf}}} + \frac{K_{\text{ALDO,dhap}}C_{\text{gap}}}{K_{\text{ALDO,eq}}V_{\text{ALDO,blf}}} + \frac{C_{\text{fdp}}C_{\text{gap}}}{K_{\text{ALDO,gap,inh}}} + \frac{C_{\text{dhap}}C_{\text{gap}}}{K_{\text{ALDO,eq}}V_{\text{ALDO,blf}}}} \tag{12}$$

Triosephosphate isomerase:

$$r_{\text{TIS}} = \frac{r_{\text{TIS}}^{\max}\left(C_{\text{dhap}} - \frac{C_{\text{gap}}}{K_{\text{TIS,eq}}}\right)}{K_{\text{TIS,dhap}}\left(1 + \frac{C_{\text{gap}}}{K_{\text{TIS,gap}}}\right) + C_{\text{dhap}}} \tag{13}$$

Glyceraldehyde 3-phosphate dehydrogenase:

$$r_{\text{GAPDH}} = \frac{r_{\text{GADPH}}^{\max}\left(C_{\text{gap}}C_{\text{nad}} - \frac{C_{\text{pgp}}C_{\text{nadh}}}{K_{\text{GAPDH,eq}}}\right)}{\left(K_{\text{GAPDH,gap}}\left(1 + \frac{C_{\text{pgp}}}{K_{\text{GAPDH,pgp}}}\right) + C_{\text{gap}}\right)\left(K_{\text{GAPDH,nad}}\left(1 + \frac{C_{\text{nadh}}}{K_{\text{GAPDH,nadh}}}\right) + C_{\text{nad}}\right)} \tag{14}$$

Phosphoglycerate kinase:

$$r_{\text{PGK}} = \frac{r_{\text{PGK}}^{\max}\left(C_{\text{adp}}C_{\text{pgp}} - \frac{C_{\text{atp}}C_{\text{3pg}}}{K_{\text{PGK,eq}}}\right)}{\left(K_{\text{PGK,adp}}\left(1 + \frac{C_{\text{atp}}}{K_{\text{PGK,atp}}}\right) + C_{\text{adp}}\right)\left(K_{\text{PGK,pgp}}\left(1 + \frac{C_{\text{3pg}}}{K_{\text{PGK,3pg}}}\right) + C_{\text{pgp}}\right)} \tag{15}$$

Phosphoglycerate mutase:

$$r_{\text{PGluMu}} = \frac{r_{\text{PGluMu}}^{\max}\left(C_{\text{3pg}} - \frac{C_{\text{2pg}}}{K_{\text{PGluMu,eq}}}\right)}{K_{\text{PGluMu,3pg}}\left(1 + \frac{C_{\text{2pg}}}{K_{\text{PGluMu,2pg}}}\right) + C_{\text{3pg}}} \tag{16}$$

Enolase:

$$r_{\text{ENO}} = \frac{r_{\text{ENO}}^{\max}\left(C_{\text{2pg}} - \frac{C_{\text{pep}}}{K_{\text{ENO,eq}}}\right)}{K_{\text{ENO,2pg}}\left(1 + \frac{C_{\text{pep}}}{K_{\text{ENO,pep}}}\right) + C_{\text{2pg}}} \tag{17}$$

Pyruvate kinase:

$$r_{\text{PK}} = \frac{r_{\text{PK}}^{\max} C_{\text{pep}}\left(\frac{C_{\text{pep}}}{K_{\text{PK,pep}}} + 1\right)^{(n_{\text{PK}}-1)} C_{\text{adp}}}{K_{\text{PK,pep}}\left(L_{\text{PK}}\left(\frac{1+\frac{C_{\text{atp}}}{K_{\text{PK,atp}}}}{\frac{C_{\text{fdp}}}{K_{\text{PK,fdp}}}+\frac{C_{\text{amp}}}{K_{\text{PK,amp}}}+1}\right)^{n_{\text{PK}}} + \left(\frac{C_{\text{pep}}}{K_{\text{PK,pep}}} + 1\right)^{n_{\text{PK}}}\right)\left(C_{\text{adp}} + K_{\text{PK,adp}}\right)} \tag{18}$$

Pyruvate dehydrogenase:

$$r_{\text{PDH}} = \frac{r_{\text{PDH}}^{\max} C_{\text{pyr}}^{n_{\text{PDH}}}}{K_{\text{PDH,pyr}} + C_{\text{pyr}}^{n_{\text{PDH}}}} \tag{19}$$

Table IV. Continued

PEP carboxylase:

$$r_{\text{PEPCxylase}} = \frac{r_{\text{PEPCxylase}}^{\max} C_{\text{pep}} \left(1 + \left(\frac{C_{\text{fdp}}}{K_{\text{PEPCxylase,fdp}}}\right)^{n_{\text{PEPCxylase,fdp}}}\right)}{K_{\text{PEPCxylase,pep}} + C_{\text{pep}}} \tag{20}$$

Phosphoglucomutase:

$$r_{\text{PGM}} = \frac{r_{\text{PGM}}^{\max} \left(C_{\text{g6p}} - \frac{C_{\text{g1p}}}{K_{\text{PGM,eq}}}\right)}{K_{\text{PGM,g6p}} \left(1 + \frac{C_{\text{g1p}}}{K_{\text{PGM,g1p}}}\right) + C_{\text{g6p}}} \tag{21}$$

Glucose 1-phosphate adenyltransferase:

$$r_{\text{G1PAT}} = \frac{r_{\text{G1PAT}}^{\max} C_{\text{g1p}} C_{\text{atp}} \left(1 + \left(\frac{C_{\text{fdp}}}{K_{\text{G1PAT,fdp}}}\right)^{n_{\text{G1PAT,fdp}}}\right)}{(K_{\text{G1PAT,glp}} + C_{\text{g1p}})(K_{\text{G1PAT,atp}} + C_{\text{atp}})} \tag{22}$$

Ribose phosphate pyrophosphokinase:

$$r_{\text{RPPK}} = \frac{r_{\text{RPPK}}^{\max} C_{\text{rib5p}}}{K_{\text{RPPK,rib5p}} + C_{\text{rib5p}}} \tag{23}$$

Glycerol 3-phosphate-dehydrogenase:

$$r_{\text{G3PDH}} = \frac{r_{\text{G3PDH}}^{\max} C_{\text{dhap}}}{K_{\text{G3PDH,dhap}} + C_{\text{dhap}}} \tag{24}$$

Serine synthesis:

$$r_{\text{SerSynth}} = \frac{r_{\text{SerSynth}}^{\max} C_{\text{3pg}}}{K_{\text{SerSynth,3pg}} + C_{\text{3pg}}} \tag{25}$$

Mureine synthesis:

$$r_{\text{MurSynth}} = r_{\text{MurSynth}}^{\max} \tag{26}$$

DAHP synthase:

$$r_{\text{DAHPS}} = \frac{r_{\text{DAHPS}}^{\max} C_{\text{e4p}}^{n_{\text{DAHPS,e4p}}} C_{\text{pep}}^{n_{\text{DAHPS,pep}}}}{(K_{\text{DAHPS,e4p}} + C_{\text{e4p}}^{n_{\text{DAHPS,e4p}}})(K_{\text{DAHPS,pep}} + C_{\text{pep}}^{n_{\text{DAHPS,pep}}})} \tag{27}$$

Tryptophan synthesis:

$$r_{\text{TrpSynth}} = r_{\text{TrpSynth}}^{\max} \tag{28}$$

Methionine synthesis:

$$r_{\text{MetSynth}} = r_{\text{MetSynth}}^{\max} \tag{29}$$

Glucose-6-phosphate dehydrogenase:

$$r_{\text{G6PDH}} = \frac{r_{\text{G6PDH}}^{\max} C_{\text{g6p}} C_{\text{nadp}}}{(C_{\text{g6p}} + K_{\text{G6PDH,g6p}}) \left(1 + \frac{C_{\text{nadph}}}{K_{\text{G6PDH,nadph,g6pinh}}}\right) \left(K_{\text{G6PDH,nadp}} \left(1 + \frac{C_{\text{nadph}}}{K_{\text{G6PDH,nadph,nadpinh}}}\right) + C_{\text{nadp}}\right)} \tag{30}$$

6-phosphogluconate dehydrogenase:

$$r_{\text{PGDH}} = \frac{r_{\text{PGDH}}^{\max} C_{\text{6pg}} C_{\text{nadp}}}{(C_{\text{6pg}} + K_{\text{PGDH,6pg}}) \left(C_{\text{nadp}} + K_{\text{PGDH,nadp}} \left(1 + \frac{C_{\text{nadph}}}{K_{\text{PGDH,nadph,inh}}}\right) \left(1 + \frac{C_{\text{ATP}}}{K_{\text{PGDH,atp,inh}}}\right)\right)} \tag{31}$$

Ribulose phosphate epimerase:

$$r_{\text{Ru5p}} = r_{\text{Ru5p}}^{\max} \left(C_{\text{ribu5p}} - \frac{C_{\text{xyl5p}}}{K_{\text{Ru5P,eq}}}\right) \tag{32}$$

Ribose phosphate isomerase:

$$r_{\text{R5P1}} = r_{\text{R5P1}}^{\max} \left(C_{\text{ribu5p}} - \frac{C_{\text{rib5p}}}{K_{\text{R5P1,eq}}}\right) \tag{33}$$

Transketolase a:

$$r_{\text{TKa}} = r_{\text{TKa}}^{\max} \left(C_{\text{rib5p}} C_{\text{xyl5p}} - \frac{C_{\text{sed7p}} C_{\text{gap}}}{K_{\text{TKa,eq}}}\right) \tag{34}$$

Transketolase b:

$$r_{\text{TKb}} = r_{\text{TKb}}^{\max} \left(C_{\text{xyl5p}} C_{\text{e4p}} - \frac{C_{\text{f6p}} C_{\text{gap}}}{K_{\text{TKb,eq}}}\right) \tag{35}$$

Table IV. Continued

Transaldolase:

$$r_{TA} = r_{TA}^{max}\left(C_{gap}C_{sed7p} - \frac{C_{e4p}C_{f6p}}{K_{TA,eq}}\right) \tag{36}$$

Synthesis 1:

$$r_{Synth1} = \frac{r_{Synth1}^{max}C_{pep}}{K_{Synth1,pep} + C_{pep}} \tag{37}$$

Synthesis 2:

$$r_{Synth2} = \frac{r_{Synth2}^{max}C_{pyr}}{K_{Synth2,pyr} + C_{pyr}} \tag{38}$$

Parameter Estimation

The response of the metabolome due to the dynamic system excitation was used to identify the dynamic system behavior by a stepwise internalization of metabolites, similar to the method proposed by Rizzi et al. (1997). For estimation of unbalanced metabolite concentrations in the submodels used for the stepwise identification of parameters, the time course of unbalanced metabolite concentrations were fitted with analytical functions (Rizzi et al., 1997; Vaseghi et al., 1999). The software packages ACSL (integration procedure: Gear algorithm; Mitchell and Gauthier, Concord, MA) and OPTDESX (optimization strategy: simulated annealing, Design Synthesis, Inc., Orem, UT) were applied for the estimation of the kinetic parameters.

RESULTS AND DISCUSSION

Figures 5 and 6 compare the measured data with predictions from the model using the parameters in Table V. The culture conditions are listed in Table VII.
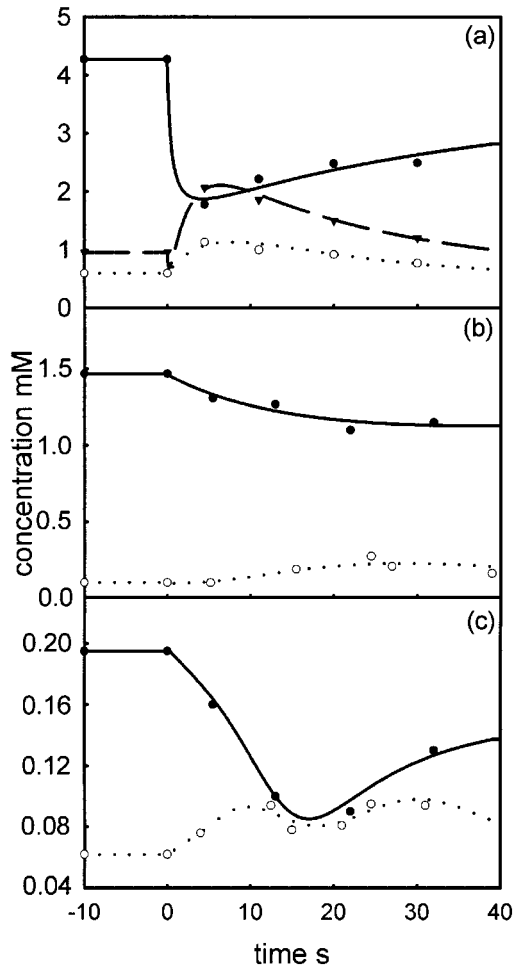
Figure 4. Analytical function graphs for cometabolites. (a) Solid line: atp; dotted line: adp; dashed line: amp. (b) Solid line: nad; dotted line: nadh. (c) Solid line: nadp; dotted line: nadph. The points represent experimental data. (a) (●) atp; (○) adp; and (▼) amp. (b) (●) nad and (○) nadh. (c) (●) nadp and (○) nadph.

Table V. Steady-state concentrations.

| Metabolite		Concentration [mM]
Glucose[extracellular]	measured	0.0556
g6p	measured	3.48
f6p	measured	0.60
fdp	measured	0.272
gap	measured	0.218
dhap	estimated	0.167
pgp	estimated	0.008
3pg	estimated	2.13
2pg	estimated	0.399
pep	measured	2.67
pyr	measured	2.67
6pg	measured	0.808
ribu5p	estimated	0.111
xyl5p	estimated	0.138
sed7p	estimated	0.276
rib5p	estimated	0.398
e4p	estimated	0.098
glp	measured	0.653
amp	measured	0.955
adp	measured	0.595
atp	measured	4.27
nadp	measured	0.195
nadph	measured	0.062
nad	measured	1.47
nadh	measured	0.1
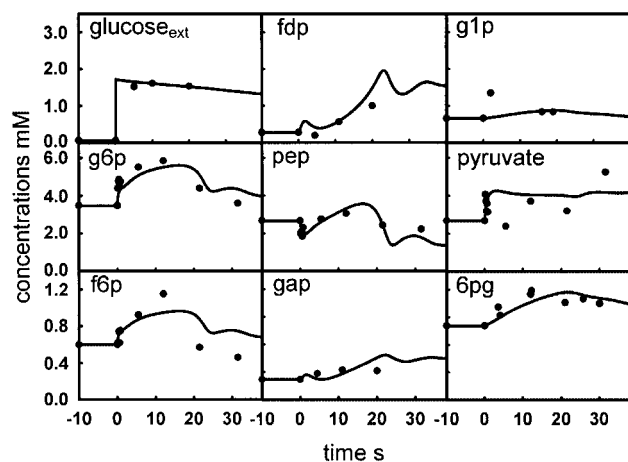
Figure 5. Comparison between experimental data (●) (maximal measurement error 20%) and model simulations (lines) after a glucose pulse (time zero) in a steady-state culture.

The model fits the observed trends for most metabolites in the second time span (experimental data from manual sampling after pulsing the glucose into the fermentor) and millisecond time scale (stopped-flow sampling). The remaining deviations between model predictions and experimental data show the present limitations in comprehensive modeling based on mechanistic rate equations. A critical assessment of this comparison, however, should also consider the experimental errors of the measured metabolites. On the other hand, these deviations also indicate the sensitivity of a complex interacting system with respect to uncertainties in its detailed structure, which cannot be compensated by parameter fitting.

The largest deviations between measured and predicted values were found for the intracellular pyruvate concentrations. Neither changing the kinetic expressions for the enzymes influencing the dynamics of the pool nor variation of parameters resulted in an improvement of the fit.

Some representative examples of the dynamics of the reaction rates are depicted in Figure 7. The sharp increase in the PTS rate (Fig. 7a) after the pulse results from the high glucose concentration, followed by a very rapid drop due to an increase in the g6p level and a decrease of the pep:pyr ratio. The PTS rate stabilizes on an elevated level, but distinctly below the maximum.

The PGI and the PFK rates follow the same pattern (Fig. 7b,c). PGI is a near-equilibrium reaction and therefore closely linked to the dynamics of PFK, which in turn is regulated by its effectors AMP, ADP, and PEP. Similar to the observations in *Saccharomyces cerevisiae* (Vaseghi et al., 1999), the dynamics of G6PDH are determined mainly by the inhibition by NADPH. The PDH rate (Fig. 7f) follows the concentration of pyruvate. The dynamics of glucose-1-phosphate adenyltransferase (G1PAT) and PEP-carboxylase (PEPCxylase) are strongly influenced by the activation through FDP.
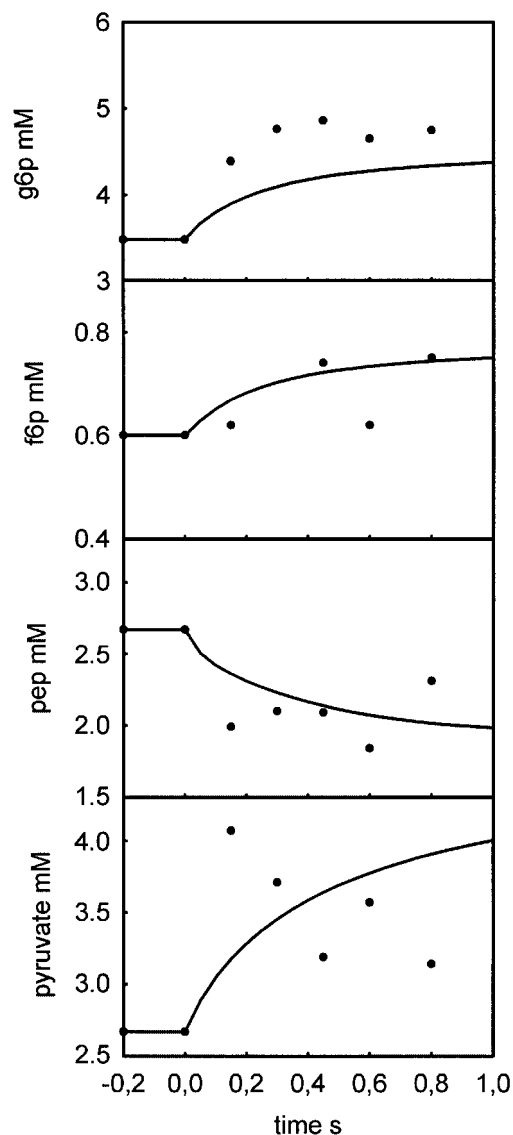

Figure 6. Comparison between experimental data (●) obtained with stopped-flow techniques and model simulations (lines) after a glucose pulse (time zero) in a steady-state culture.

Stability Analysis

A stable steady state is an essential prerequisite for a mathematical model of living cells as well as for application of metabolic control analysis. In context with the envisaged application of the model for tasks of metabolic design it is also important to emphasize that enzymes with negligible flux control coefficients may strongly influence the stability of a steady state exposed to noise perturbation (Liu et al., 1996, 1997). As these noises are common in industrial practice, careful analysis of the stability of redesigned "in silico" strains should be mandatory (Mauch et al., 2001).

The simulations shown in Figure 5 do not provide evidence for the stability of the model. The apparent stability of the system might be a wrong assumption because of instabilities in the long-term behavior or

Table VI. Analytical function for cometabolites [atp, adp, amp, nadp(h), and nad(h)].

$$C_{atp} = 4.27 - 4.163 \frac{t}{0.657 + 1.43t + 0.364t^2}$$

$$C_{adp} = 0.582 + 1.73(2.731^{-0.15t})(0.12t + .000214t^3)$$

$$C_{amp} = 0.123 + 7.25 \frac{t}{7.25 + 1.47t + 0.17t^2} + 1.073 \frac{t}{1.29 + 8.05t}$$

$$C_{nadph} = 0.062 + 0.332(2.718^{-0.464t})(0.0166t^{1.58} + 0.000166t^{4.73} + 1.13_{10}^{-10}t^{7.89} + 1.36_{10}^{-13}t^{11.0} + 1.23_{10}^{-16}t^{14.2})$$

$$C_{nadp} = 0.159 + 0.00554 \frac{t}{2.8 + 0.271t + 0.01t^2} + 0.182 \frac{t}{4.81 + 0.526t}$$

$$C_{nadh} = 0.0934 + 0.0011(2.371^{-0.123t})(0.844t + 0.104t^3)$$

$$C_{nad} = 1.314 + 1.314(2.73^{(-0.0435t-0.342)}) - \frac{(t + 7.871)(2.73^{(-0.0218t-0.171)})}{8.481 + t}$$

unexpected responses to alternative perturbations. As shown in Figure 5, not all concentrations return to the steady state within the simulated time scale, which is determined by the available data for the unbalanced cometabolites. A reliable prediction of the stability of the system should therefore rest on the investigation of the eigenvalues of the Jacobian matrix.

Beyond proof of stability, the eigenvalues also contain information on how fast a deviation from a given steady state will decline. The time constants of the decline have been defined as the reciprocal absolute values of the real parts of the eigenvalues (Heiurich and Schuster, 1996). In the dynamic model presented in this article, the time constants range from $t_{min} = 0.29$ ms to $t_{max} = 85$ s. The time constant for the terms μC_i (dilution by growth) in Eq. (1) is 10 h, four orders of magnitude higher than the largest time constant of the system. The return to steady state of the system is thus much faster than the dilution effects. The wide range of time constants might give clues for future model simplifications, although relationships between time constants and the control hierarchy are restricted to unbranched pathways (Delgado and Liao, 1995).

In addition, a pair of conjugate complex eigenvalues point out the ability of the system to oscillate. Oscillations are due to one natural frequency, which can be calculated from the imaginary part, Im, of the complex
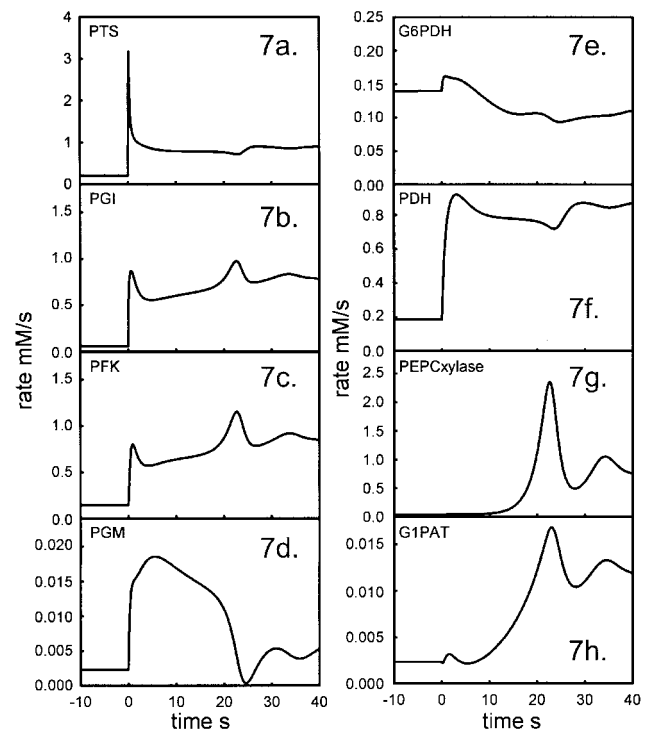
Table VII. Culture parameters.

$$D = 0.278e - 4 \text{ s}^{-1}$$

$$C_{glc}^{feed} = 111.1 \text{ m}M$$

$$C_x = 8.7 \text{ g DW L}^{-1} \text{ culture volume}$$

$$\rho_x = 564 \text{ g DW L}^{-1} \text{ cell volume}$$

$$\mu = 0.278e - 4 \text{ s}^{-1}$$

eigenvalues λ by $Im(\lambda)/2\pi$. For the system presented, the natural frequency from the eigenvalues is $f_1 = 0.013$ s^{-1}, synonymous with a period of 78 s. The calculated period not only describes the experimentally observed dynamic behavior, it is also of the same order of magnitude as the oscillations described in the experimental work of Schaefer et al. (1999).

Control Characteristics

The main field of application addressed by our dynamic model is an investigation of promising strategies for

Figure 7. Time courses of some simulated kinetic rates of the model after a glucose pulse.
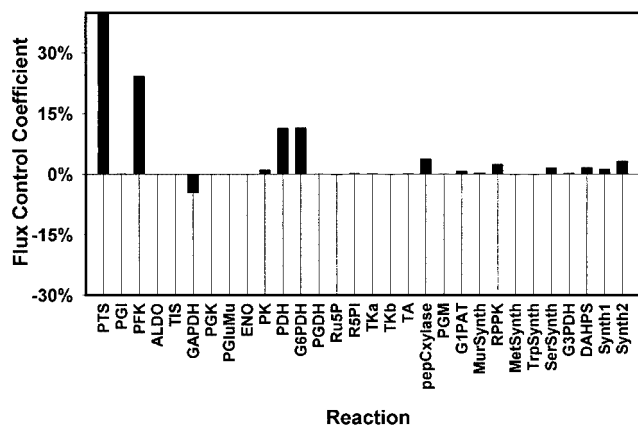
Figure 8. Flux control coefficients (FCC) of the reactions in the system on the glucose uptake by the phosphotransferase system.

improvement of microbial production processes. Thus, provision is made for optimization of selected production rates by computer-aided design (Mauch et al., 2001). As a preliminary step, flux control coefficients (FCC) on the glucose uptake by the phosphotransferase system were determined from the dynamic model. The results of these calculations are summarized in Figure 8.

The highest control on glucose uptake is exerted by the PTS as indicated by FCC = 0.42. This outstanding role for the PTS was expected, as glucose uptake is irreversible and represents the first step in the model network, thus not depending on a potential precedent reaction. Nevertheless, there are further enzymes that exercise considerable control on glucose uptake, primarily on the basis of inhibitory effects on the PTS. According to the FCCs, the most important of these enzymes is the PFK (FCC of 0.24). It degrades F6P, which is in near equilibrium with the PTS inhibitor G6P because of the fast reversible reaction of PGI. For equivalent reasons, G6PDH exerts a high control on glucose uptake (FCC of 0.11) as it is a G6P-consuming reaction. The PTS is also inhibited by its coproduct, pyruvate. Accordingly, the pyruvate-degradating enzyme, PDH, is fourth in the hierarchy of PTS flux control (FCC = 0.11). Surprisingly, under the conditions given in this model, the supply of the PTS cosubstrate PEP, is not decisive for glucose uptake, as indicated, for example, by the low FCC of PK (i.e., 0.01).

Because control coefficients are defined for infinitesimal perturbations, their predictive character for effects of large changes (e.g., in enzyme content) is limited.

Table VIII. Kinetic parameters (initial values and optimized values).

Enzyme activities	Parameters	Parameter values before optimization [ref]	Optimized parameter values
PTS	$K_{PTS,a1}$	1 mM [arbitrary]	3082.3 mM
	$K_{PTS,a2}$	0.01 mM[a]	0.01 mM
	$K_{PTS,a3}$	1 [arbitrary]	245.3
	$K_{PTS,g6p}$	0.5 mM[b]	2.15 mM
	$n_{PTS,g6p}$	4 [arbitrary]	3.66
PGI	$K_{PGI,g6p}$	2.46 mM[c]	2.9 mM
	$K_{PGI,f6p}$	0.2 mM[d]	0.266 mM
	$K_{PGI,eq}$	0.43[e] [index]	0.1725
	$K_{PGI,g6p,6pginh}$	0.2 mM[f]	0.2 mM
	$K_{PGI,f6p,6pginh}$	0.2 mM[f]	0.2 mM
PFK	$K_{PFK,g6p,s}$	0.14 mM[g]	0.325 mM
	$K_{PFK,atp,s}$	0.16 mM[g]	0.123 mM
	$K_{PFK,adp,a}$	239 mM[h]	128 mM
	$K_{PFK,adp,b}$	0.25 mM[h]	3.89 mM
	$K_{PFK,adp,c}$	0.36 mM[h]	4.14 mM
	$K_{PFK,amp,a}$	8.74 mM[h]	19.1 mM
	$K_{PFK,amp,b}$	0.01 mM[h]	3.2 mM
	L_{PFK}	4,000,000[i]	5629067
	n_{PFK}	4[i]	11.1
ALDO	$K_{ALDO,fdp}$	0.133 mM[j]	1.75 mM
	$K_{ALDO,dhap}$	0.088 mM[j]	0.088 mM
	$K_{ALDO,gap}$	0.088 mM[j]	0.088 mM
	$K_{ALDO,gap,inh}$	0.6 mM[j]	0.6 mM
	$V_{ALDO,blf}$	2[j]	2
	$K_{ALDO,eq}$	0.1–0.14 mM[j,e]	0.144 mM
TIS	$K_{TIS,dhap}$	2.8 mM[j]	2.8 mM
	$K_{TIS,gap}$	0.3 mM[j]	0.3 mM
	$K_{TIS,eq}$	0.04[j]	1.39
GAPDH	$K_{GAPDH,gap}$	0.15 mM[k]	0.683 mM
	$K_{GAPDH,pgp}$	0.1 mM[k]	0.0000104 mM
	$K_{GAPDH,nad}$	0.45 mM[k]	0.252 mM
	$K_{GAPDH,nadh}$	0.02 mM[k]	1.09 mM
	$K_{GAPDH,eq}$	0.63[e]	0.63

Table VIII. Continued

Enzyme activities	Parameters	Parameter values before optimization [ref]	Optimized parameters values
PGK	$K_{PGK,pgp}$	0.006 mM[l]	0.0468 mM
	$K_{PGK,3pg}$	0.17 mM[m]	0.473 mM
	$K_{PGK,adp}$	0.18 mM[n]	0.185 mM
	$K_{PGK,atp}$	0.24 mM[o]	0.653 mM
	$K_{PGK,eq}$	1800[p]	1934.4
PGluMu	$K_{PGluMu,3pg}$	0.2 mM[q]	0.2 mM
	$K_{PGluMu,2pg}$	0.369 mM[r]	0.369 mM
	$K_{PGluMu,eq}$	0.1–0.187[e,k]	0.188
ENO	$K_{ENO,2pg}$	0.1 mM[s]	0.1 mM
	$K_{ENO,pep}$	0.135 mM[t]	0.135 mM
	$K_{ENO,eq}$	4–6.7[k,t]	6.73 mM
PK	$K_{PK,pep}$	0.31 mM[u]	0.31 mM
	$K_{PK,adp}$	0.26 mM[u]	0.26 mM
	$K_{PK,atp}$	22.5 mM[u]	22.5 mM
	$K_{PK,fdp}$	0.19 mM[u]	0.19 mM
	$K_{PK,amp}$	0.2 mM [arbitrary]	0.2 mM
	L_{PK}	1000[u]	1000
	n_{PK}	4[u]	4
PDH	$K_{PDH,pyr}$	0.11 mM[v]	1159 mM
	n_{PDH}	1[v]	3.68
PepCxylase	$K_{PepCxylase,pep}$	1 mM [arbitrary]	4.07 mM
	$K_{PepCxylase,fdp}$	1 mM [arbitrary]	0.7 mM
	$n_{PepCxylase,fdp}$	4 [arbitrary]	4.21
PGM	$K_{PGM,g6p}$	0.02 mM[w]	1.038 mM
	$K_{PGM,g1p}$	0.008 mM[w]	0.0136 mM
	$K_{PGM,eq}$	0.142 mM[w]	0.196
G1PAT	$K_{G1PAT,g1p}$	0.12 mM[x]	3.2 mM
	$K_{G1PAT,atp}$	1.3 mM[x]	4.42 mM
	$K_{G1PAT,fdp}$	0.068 mM[x]	0.119 mM
	$n_{G1PAT,fdp}$	2[x]	1.20
RPPK	$K_{RPPK,rib5p}$	0.1 mM [arbitrary]	0.1 mM
G3PDH	$K_{G3PDH,dhap}$	1 mM [arbitrary]	1 mM
SerSynth	$K_{SerSynth,3pg}$	1 mM [arbitrary]	1 mM
Synth1	$K_{Synth1,pep}$	1 mM [arbitrary]	1 mM
Synth2	$K_{Synth2,pyr}$	1 mM [arbitrary]	1 mM
DAHPS	$K_{DAHPS,e4p}$	0.035 mM[y]	0.035 mM
	$K_{DAHPS,pep}$	0.0053 mM[y]	0.0053 mM
	$n_{DAHPS,e4p}$	2.6[y]	2.6
	$n_{DAHPS,pep}$	2.2[y]	2.2
G6PDH	$K_{G6PDH,g6p}$	0.07 mM[z]	14.4 mM
	$K_{G6PDH,nadp}$	0.015 mM[z]	0.0246 mM
	$K_{G6PDH,nadph,nadphinh}$	0.01 mM[z]	0.01 mM
	$K_{G6PDH,nadph,g6pinh}$	0.18 mM[z]	6.43 mM
PGDH	$K_{PGDH,6pg}$	0.1 mM[aa]	37.5 mM
	$K_{PGDH,nadp}$	0.028 mM[aa]	0.0506 mM
	$K_{PGDH,nadph,inh}$	0.01 mM[aa]	0.0138 mM
	$K_{PGDH,atp,inh}$	3 mM[aa]	208 mM
Ru5P	$K_{Ru5P,eq}$	1.4[ab]	1.4
R5PI	$K_{R5PI,eq}$	4.0[ab]	4.0
TKa	$K_{TKa,eq}$	1.2[ab]	1.2
TKb	$K_{TKb,eq}$	10.0[ab]	10.0
TA	$K_{TA,eq}$	1.05[ab]	1.05

[a]Notley-McRobb et al. (1997); [b]Kaback (1969); [c]Takama and Nosoh (1980); [d]Dykhuizen and Hartl (1983); [e]Pettersson (1990); [f]Schreyer and Bock (1980); [g]Deville-Bonne et al., (1991); [h]Rizzi et al. (1997); [i]Diag Ricci (1999); [j]Babul et al. (1993); [k]Bakker et al. (1997); [l]Lavoinne et al. (1983); [m]Schmidt et al. (1995); [n]Molnar and Vas (1993); [o]Fifis and Scopes (1978); [p]Ni and Savageau, (1996); [q]Britton et al. (1972); [r]Grana et al. (1989); [s]Spring and Wold (1971); [t]Duggleby, (1994); [u]Boiteux et al. (1983); [v]Yi et al. (1996); [w]Lowry and Passonneau (1969); [x]Preiss et al. (1975); [y]Akowski and Bauerle (1970); [z]Sanwal (1970); [aa]Orozco de Silva (1979); [ab]Vaseghi et al. (1999).

However, they point at properties in the reaction network that represent promising areas for optimization.

CONCLUSIONS

A dynamic model of glycolysis and the pentose-phosphate pathway in *Escherichia coli* has been designed and validated with measured metabolite concentrations at transient conditions to support the exploration of the central carbon metabolism, as a supplier of precursors. The model structure is the first that links the kinetics of the important sugar transporter PTS with the central carbon metabolism for these bacteria. The strong nonlinear feedback/feedforward link between the PTS and glycolytic pool concentrations of PEP and Pyr might be considered an outstanding candidate for a "structural determinant" in dynamic modeling.

The ability of the model to capture the experimentally observed dynamic behavior of metabolites gives strong credence to the application for metabolic design tasks. The model is also capable of describing the oscillations observed in experiments with *Escherichia coli* (Schaefer et al., 1999). This structural property of the nonlinear system provides further confidence in the predictive capabilities of the model.

In a first step toward application of rational design, the model has been applied to the concepts of metabolic control analysis (MCA). It was shown that, for glucose uptake, the flux control is shared between the glucose uptake system PTS itself and enzymes that relieve the uptake system by degradation of the PTS inhibitors G6P and pyruvate.

Ongoing research is directed toward a more comprehensive approach for application in the production of aromatic compounds via nonlinear optimization strategies for modulation of enzyme activities. This approach has already been applied successfully for maximizing the flux from glucose to ethanol in *Saccharomyces cerevisiae* (Mauch et al., 2001).

NOMENCLATURE

Enzymes

AlaSynth	alanine synthesis
ALDO	aldolase
ChoSynth	chorismate synthesis
DAHPS	DAHP synthases
DipimSynth	diaminopimelate synthesis
ENO	enolase
G1PAT	glucose-1-phosphate adenyltransferase
G3PDH	glycerol-3-phosphate dehydrogenase
G6PDH	glucose-6-phosphate dehydrogenase
GAPDH	glyceraldehyde-3-phosphate dehydrogenase
IleSynth	isoleucine synthesis
MetSynth	methionine synthesis
MurSynth	mureine synthesis
PFK	phosphofructokinase
PGDH	6-phosphogluconate dehydrogenase
PGI	glucose-6-phosphate isomerase
PGK	phosphoglycerate kinase
PGluMu	phosphoglycerate mutase
PDH	pyruvate dehydrogenase
PEPCxylase	PEP carboxylase
PGM	phosphoglucomutase
PK	pyruvate kinase
ppp	pentose-phosphate pathway
PTS	phosphotransferase system
R5PI	ribose-phosphate isomerase
RPPK	ribose-phosphate pyrophosphokinase
Ru5P	ribulose-phosphate epimerase
Synth1	synthesis 1
Synth2	synthesis 2
TA	transaldolase
TIS	triosephosphate isomerase
TKa	transketolase, reaction a
TKb	transketolase, reaction b
TrpSynth	tryptophan synthesis

Metabolites

2pg	2-phosphoglycerate
3pg	3-phosphoglycerate
6pg	6-phosphogluconate
accoA	acetyl-coenzyme A
adp	adenosindiphosphate
aicar	5-amino-4-imidazolecarboxamideribotide
akg	α-ketoglutarate
aki	α-ketoisovalerate
amp	adenosinmonophosphate
arg	arginine
asn	asparagine
asp	aspartate
atp	adenosintriphosphate
carp	carbamoylphosphate
cdp	cytideindiphosphate
cho	chorismate
cmp	cytideinmonophosphate
co$_2$	carbondioxide
coA	coenzyme A
ctp	cytideintriphosphate
cys	cysteine
dala	D-alanine
damp	deoxyadenosinmonophosphate
dcmp	deoxycytideinmonophosphate
dglu	D-glutamate
dgmp	deoxyguanosinmonophosphate
dhap	dihydroxyacetonephosphate
dna	deoxyribonucleic acid
dtmp	deoxythymidinmonophosphate
dipim	diaminopimelate
e4p	erythrose-4-phosphate
etamp	phosphatidyl-ethanolamine
f6p	fructose-6-phosphate
fad	flavin-adenine-dinucleotide, oxidized
fadh2	flavin-adenine-dinucleotide, reduced
fatty$_{n,i}$	fatty acid containing n carbon atoms and i double bonds
fdp	fructose-1,6-bisphosphate
fthf	formyltetrahydrofolate
fum	fumarate
g1p	glucose-1-phosphate
g6p	glucose-6-phosphate
gap	glyceraldehyde-3-phosphate
glc	glucose
gln	glutamine
gly	glycine
glycp	glycerol-3-phosphate

gmp	guanosinmonophosphate
h	proton
h$_2$o	water
h$_c$	proton, in cytosol
h$_E$	proton, extracellular
his	histidine
hom	homoserine
ile	isoleucine
imp	inosinmonophosphate
isocit	isocitrate
kival	α-ketoisovalerate
lala	ʟ-alanine
leu	leucine
lglu	ʟ-glutamate
lys	lysine
mal	malate
met	methionine
methf	methylentetrahydrofolate
mythf	methyltetrahydrofolate
murunit	subunit of mureine
nad	diphosphopyridindinucleotide, oxidized
nadh	diphosphopyridindinucleotide, reduced
nadp	diphosphopyridindinucleotide-phosphate, oxidized
nadph	diphosphopyridindinucleotide-phosphate, reduced
nh4	ammonium
O$_2$	oxygen
oac	oxaloacetate
orn	ornithine
p	inorganic phosphate
pep	phosphoenolpyruvate
phe	phenylalanine
pgp	1,3-diphosphoglycerate
pro	proline
prpp	phosphoribosylpyrophosphate
pyr	pyruvate
Q	ubiquinone, oxidized
Qh$_2$	ubiquinone, reduced
Rib5p	ribose-5-phosphate
ribu5p	ribulose-5-phosphate
rna	ribonucleic acid
sed7p	sedoheptulose-7-phosphate
ser	serine
SO$_4$	sulfate
suc	succinate
succoA	succinyl-coenzyme A
thf	tetrahydrofolate
thr	threonine
trp	tryptophan
tyr	tyrosine
udp	uridindiphosphate
ump	uridinmonophosphate
utp	uridintriphosphate
val	valine
xyl5p	xylulose-5-phosphate

APPENDIX

List of reaction stoichiometries of the steady-state flux model according to ECOCYC (Karp et al., 1999) and Neidhardt et al. (1996). The cometabolites amp, adp,

and atp are treated as external. Substances crossing the boundaries of the system:

Glucose, acetate, biomass, o$_2$, co$_2$, protons, h$_2$o

by symport:
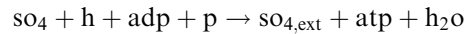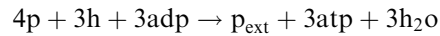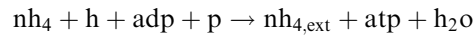
$$nh_4 + h + adp + p \rightarrow nh_{4,ext} + atp + h_2o$$
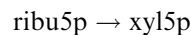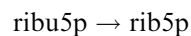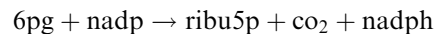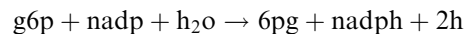$$4p + 3h + 3adp \rightarrow p_{ext} + 3atp + 3h_2o$$
$$so_4 + h + adp + p \rightarrow so_{4,ext} + atp + h_2o$$
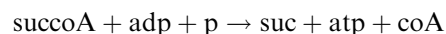
Phosphotransferase system:

$$glucose + pep \rightarrow g6p + pyr$$

Embden–Meyerhof–Parnas pathway:

$$g6p \rightarrow f6p$$
$$f6p + atp \rightarrow fdp + adp + h$$
$$fdp \rightarrow gap + dhap$$
$$dhap \rightarrow gap$$
$$gap + nad + adp + p \rightarrow 3pg + atp + nadh + h$$
$$3pg \rightarrow pep + h_2o$$
$$pep + adp + h \rightarrow pyr + atp$$
$$pyr + nad + coA \rightarrow accoA + nadh + co_2$$

Pentose-phosphate pathway:

$$g6p + nadp + h_2o \rightarrow 6pg + nadph + 2h$$
$$6pg + nadp \rightarrow ribu5p + co_2 + nadph$$
$$ribu5p \rightarrow rib5p$$
$$ribu5p \rightarrow xyl5p$$
$$rib5p + xyl5p \rightarrow sed7p + gap$$
$$sed7p + gap \rightarrow f6p + e4p$$
$$xyl5p + e4p \rightarrow f6p + gap$$
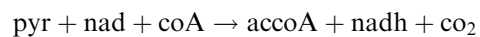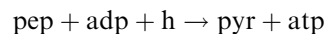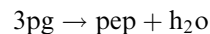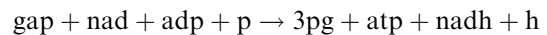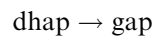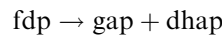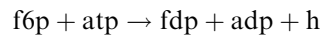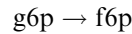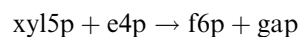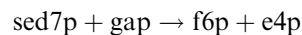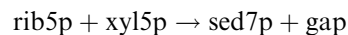
Tricarboxylic acid cycle:

$$oac + accoA + h_2o \rightarrow isocit + coA + h$$
$$isocit + nad \rightarrow akg + nadh + co_2$$
$$akg + coA + nad \rightarrow succoA + nadh + co_2$$
$$succoA + adp + p \rightarrow suc + atp + coA$$
$$suc + fad \rightarrow fum + fadh_2$$
$$fum + h_2o \rightarrow mal$$
$$mal + nad \rightarrow oac + nadh + h$$

Phosphoenolpyruvate carboxylase:

$$pep + co_2 + h_2o \rightarrow oac + p + h$$

Amino acid synthesis:

$$pyr + lglu \rightarrow lala + akg$$
$$lala \rightarrow dala$$
$$2h_2o + co_2 + gln + 2atp \rightarrow carp + lglu + p + 2adp + 3h$$
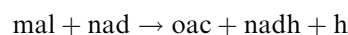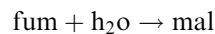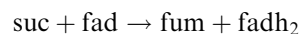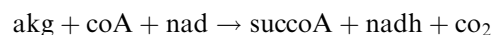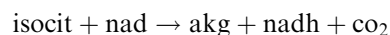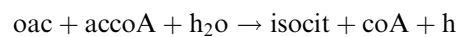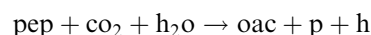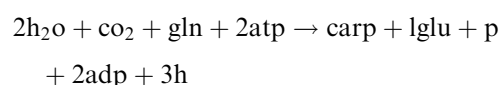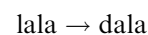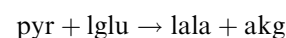
2lglu + accoA + atp + nadph + h$_2$o → orn + akg
  + coA + adp + p + nadp + acetate + h

acetate + atp + coA → accoA + adp + p

orn + carp + asp + atp + h$_2$o → arg + fum + amp
  + 3p + 2h

asp + nh$_4$ + atp + h$_2$o → asn + 2h + amp + 2p

oac + lglu → asp + akg

so$_4$ + 2atp + 4nadph + 2h → sulfide + 4nadp + 2adp
  + 2p + 2h$_2$o

ser + accoA + sulfide + h → cys + coA + acetate

nh$_4$ + akg + nadph + h → lglu + nadp + h$_2$o

lglu → dglu

lglu + nh$_4$ + atp → gln + adp + p + h

ser + thf → gly + methf + h$_2$o

prpp + gln + atp + 2nad + 5h$_2$o → his + aicar + akg
  + 2nadh + 7h + 5p

asp + atp + 2nadph + 2h → hom + adp + p + 2nadp

thr + pyr + nadph + lglu + 2h → ile + nh$_4$ + nadp
  + h$_2$o + co$_2$ + akg

hom + succoA + cys + mythf + h$_2$o → met + coA
  + suc + pyr + nh$_4$ + h + thf

asp + pyr + lglu + succoA + atp + 2nadph + h
  → dipim + akg + suc + coA + adp + 2nadp + p

2pyr + nadph + 2h → aki + co$_2$ + nadp + h$_2$o

aki + lglu + accoA + h$_2$o + nad → leu + akg + coA
  + nadh + h + co$_2$

dipim + h → lys + co$_2$

2pep + e4p + nadph + atp → cho + adp + 4p + nadp

cho + lglu + h → phe + akg + co$_2$ + h$_2$o

lglu + atp + 2nadph + 2h → pro + adp + p
  + h$_2$o + 2nadp

3pg + lglu + nad + h$_2$o → ser + akg + p + nadh + h

hom + atp + h$_2$o → thr + adp + p + h

cho + gln + prpp + ser → trp + 2p + co$_2$ + gap
  + lglu + h + pyr + h$_2$o

cho + lglu + nad → tyr + akg + co$_2$ + nadh

aki + lglu → val + akg

Nucleotide metabolism:

rib5p + atp → prpp + amp + h

prpp + 2gln + gly + 5atp + asp + fthf + 4h$_2$o + co$_2$
  → aicar + 5adp + 7p + 2lglu + thf + fum + 9h

aicar + fthf → imp + thf + h$_2$o

imp + asp + atp → amp + adp + p + fum + 2h

amp + atp → 2adp

imp + nad + atp + gln + 3h$_2$o → gmp + amp + nadh
  + 2p + 4h + lglu

carp + asp + $\frac{1}{2}$o$_2$ + prpp → ump + h$_2$o + co$_2$ + 3p

ump + atp → udp + adp

udp + atp → utp + adp

utp + gln + atp + h$_2$o → ctp + adp + p + 2h + lglu

ctp + adp → cdp + atp

cdp + adp → cmp + atp

adp + atp + nadph + h → datp + adp + h$_2$o + nadp

gmp + 2atp + nadph + h → dgtp
  + 2adp + h$_2$o + nadp

cdp + atp + nadph + h → dctp + adp + h$_2$o + nadp

udp + 3atp + 2nadph + h$_2$o + methf → dttp + 3adp
  + 2nadp + 2p + thf

Synthesis of lipid precursors

dhap + nadh + h → glycp + nad

glycp + ser + ctp + h$_2$o → etamp + cmp + co$_2$
  + 2p + h

5accoA + 4atp + 8nadph + 3h + h$_2$o → fatty$_{10,0}$
  + 5coA + 4adp + 8nadp + 4p

6accoA + 5atp + 10nadph + 4h + h$_2$o → fatty$_{12,0}$
  + 6coA + 5adp + 10nadp + 5p

5accoA + succoA + pyr + 5atp + 10nadph
  + 4h + h$_2$o → fatty$_{13,0}$ + oac + 6coA
  + 5adp + 10nadp + 5p

5accoA + succoA + pyr + 5atp + 9nadph + 3h + h$_2$o
  → fatty$_{13,1}$ + oac + 6coA + 5adp + 9nadp + 5p

7accoA + 6atp + 12nadph + 5h + h$_2$o → fatty$_{14,0}$
  + 7coA + 6adp + 12nadp + 6p

7accoA + 6atp + 11nadph + 4h + h$_2$o → fatty$_{14,1}$
  + 7coA + 6adp + 11nadp + 6p

6accoA + succoA + pyr + 6atp + 12nadph
  + 5h + h$_2$o → fatty$_{15,0}$ + oac + 7coA + 6adp
  + 12nadp + 6p

6accoA + succoA + pyr + 6atp + 11nadph
  + 4h + h$_2$o → fatty$_{15,1}$ + oac + 7coA + 6adp
  + 11nadp + 6p

8accoA + 7atp + 14nadph + 6h + h$_2$o → fatty$_{16,0}$
  + 8coA + 7adp + 14nadp + 7p

8accoA + 7atp + 13nadph + 5h + h$_2$o → fatty$_{16,1}$
  + 8coA + 7adp + 13nadp + 7p

7accoA + succoA + pyr + 7atp + 14nadph
  + 6h + h$_2$o

$$\rightarrow \text{fatty}_{17,0} + \text{oac} + 8\text{coA} + 7\text{adp} + 14\text{nadp} + 7\text{p}$$

$$7\text{accoA} + \text{succoA} + \text{pyr} + 7\text{atp} + 13\text{nadph}$$
$$+ 5\text{h} + \text{h}_2\text{o} \rightarrow \text{fatty}_{17,1} + \text{oac} + 8\text{coA} + 7\text{adp}$$
$$+ 13\text{nadp} + 7\text{p}$$

$$9\text{accoA} + 8\text{atp} + 16\text{nadph} + 7\text{h} + \text{h}_2\text{o} \rightarrow \text{fatty}_{18,0}$$
$$+ 9\text{coA} + 8\text{adp} + 16\text{nadp} + 8\text{p}$$

$$9\text{accoA} + 8\text{atp} + 15\text{nadph} + 6\text{h} + \text{h}_2\text{o} \rightarrow \text{fatty}_{18,1}$$
$$+ 9\text{coA} + 8\text{adp} + 15\text{nadp} + 8\text{p}$$

$$8\text{accoA} + \text{succoA} + \text{pyr} + 8\text{atp} + 16\text{nadph}$$
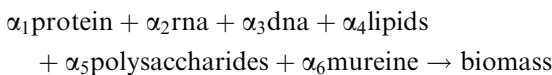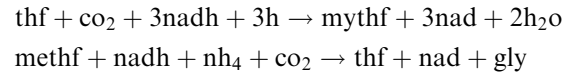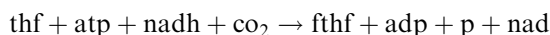$$+ 7\text{h} + \text{h}_2\text{o} \rightarrow \text{fatty}_{19,0} + \text{oac} + 9\text{coA} + 8\text{adp}$$
$$+ 16\text{nadp} + 8\text{p}$$
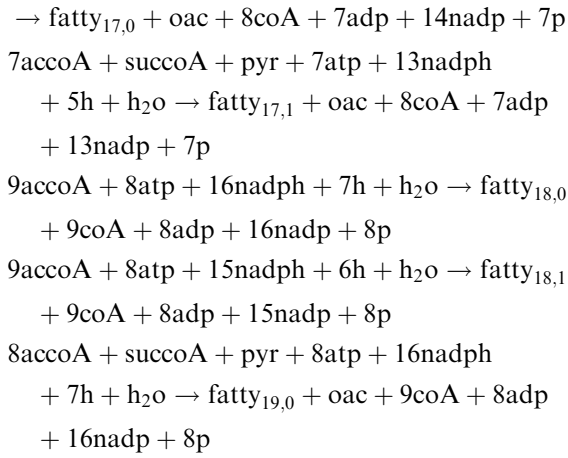
Polymerization reactions:

$$\beta_1\text{lala} + \beta_2\text{arg} + \beta_3\text{asn} + \beta_4\text{asp} + \beta_5\text{cys} + \beta_6\text{gln}$$
$$+ \beta_7\text{lglu} + \beta_8\text{gly} + \beta_9\text{his} + \beta_{10}\text{ile}+$$
$$\beta_{11}\text{leu} + \beta_{12}\text{lys} + \beta_{13}\text{met} + \beta_{14}\text{phen} + \beta_{15}\text{pro} + \beta_{16}\text{ser}$$
$$+ \beta_{17}\text{thr} + \beta_{18}\text{trp} + \beta_{19}\text{tyr}+$$
$$\beta_{20}\text{val} + \beta_{21}\text{atp} + \beta_{22}\text{h}_2\text{o} \rightarrow \text{protein} + \beta_{21}\text{adp} + \beta_{21}\text{p}$$
$$+ \beta_{21}\text{h}$$

$$\chi_1\text{amp} + \chi_2\text{cmp} + \chi_3\text{gmp} + \chi_4\text{ump} + \chi_5\text{atp} + \chi_6\text{h}_2\text{o}$$
$$\rightarrow \text{rna} + \chi_5\text{adp} + \chi_5\text{p} + \chi_5\text{h}$$

$$\varepsilon_1\text{fatty}_{10,0} + \varepsilon_2\text{fatty}_{12,0} + \varepsilon_3\text{fatty}_{13,0} + \varepsilon_4\text{fatty}_{13,1}$$
$$+ \varepsilon_5\text{fatty}_{14,0} + \varepsilon_6\text{fatty}_{14,1} + \varepsilon_7\text{fatty}_{15,0} + \varepsilon_8\text{fatty}_{15,1}$$
$$+ \varepsilon_9\text{fatty}_{16,0} + \varepsilon_{10}\text{fatty}_{16,1} + \varepsilon_{11}\text{fatty}_{17,0}$$
$$+ \varepsilon_{12}\text{fatty}_{17,1} + \varepsilon_{13}\text{fatty}_{18,0} + \varepsilon_{14}\text{fatty}_{18,1}$$
$$+ \varepsilon_{15}\text{fatty}_{19,0} + \varepsilon_{16}\text{glycp} + \varepsilon_{17}\text{etamp}$$
$$\rightarrow \text{lipid} + \varepsilon_{18}\text{h}_2\text{o}$$

$$(\phi_1 + 1)\text{g6p} + \phi_1\text{atp} + \phi_1\text{h}_2\text{o} \rightarrow \text{polysaccharides}$$
$$+ 2\phi_1\text{p} + \phi_1\text{adp} + \phi_1\text{h}$$

$$2\text{f6p} + 2\text{gln} + 2\text{accoA} + 7\text{atp} + \text{pep} + \text{nadph} + \text{lala}$$
$$+ \text{dglu} + \text{dipim} + \text{dala} + 5\text{h}_2\text{o} \rightarrow$$
$$\rightarrow \text{murunit} + 2\text{coA} + 2\text{lglu} + 6\text{adp} + \text{amp} + \text{nadp}$$
$$+ 11\text{p} + 9\text{h}$$

$$\gamma_1\text{murunit} \rightarrow \text{mureine} + \gamma_2\text{h}_2\text{o}$$

values of β_i, χ_i, δ_i, ε_i, ϕ_i, and γ_i according to the biomass composition.

Virtual biomass formation reaction:

$$\alpha_1\text{protein} + \alpha_2\text{rna} + \alpha_3\text{dna} + \alpha_4\text{lipids}$$
$$+ \alpha_5\text{polysaccharides} + \alpha_6\text{mureine} \rightarrow \text{biomass}$$

values of α_i according to the biomass composition.

Regeneration of C1-transfer cometabolites:

$$\text{thf} + \text{atp} + \text{nadh} + \text{co}_2 \rightarrow \text{fthf} + \text{adp} + \text{p} + \text{nad}$$

$$\text{thf} + \text{co}_2 + 3\text{nadh} + 3\text{h} \rightarrow \text{mythf} + 3\text{nad} + 2\text{h}_2\text{o}$$
$$\text{methf} + \text{nadh} + \text{nh}_4 + \text{co}_2 \rightarrow \text{thf} + \text{nad} + \text{gly}$$

Oxidative phosphorylation:

$$\text{nadh} + \text{h} + \text{Q} + 4\text{h}_c \rightarrow \text{Qh}_2 + \text{nad} + 4\text{h}_E$$
$$\text{fadh}_2 + \text{Q} \rightarrow \text{Qh}_2 + \text{fad}$$
$$\text{Qh}_2 + \tfrac{1}{2}\text{o}_2 + 4\text{h}_c \rightarrow \text{Q} + \text{h}_2\text{o} + 4\text{h}_E$$
$$\text{h}_E \rightarrow \text{h}_c$$
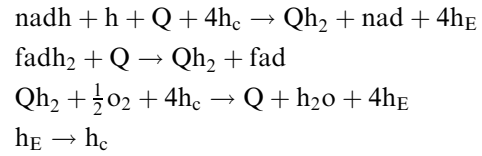
References

Akowski JP, Bauerle R. 1997. Steady-state kinetics and inhibitor binding of 3-deoxy-D-arabino-heptulosonate-7-phosphate synthase (tryptophan sensitive) from *Escherichia coli*. Biochemistry 36:15817–15822.

Babul J, Clifton D, Kretschmer M, Fraenkel DG. 1993. Glucose metabolism in *Escherichia coli* and the effect of increased amount of aldolase. Biochemistry 32:4685–4692.

Bakker BM, Michels PAM, Opperdoes FR, Westerhoff HV. 1997. Glycolysis in bloodstream from *Trypanosoma brucei* can be understood in terms of the kinetics of the glycolytic enzymes. J Biol Chem 272:3207–3215.

Bhattacharya M, Fuhrman L, Ingram A, Nickerson KW, Conway T. 1995. Single-run separation and detection of multiple metabolic intermediates by anion-exchange high-performance liquid chromatography and application to cell pool extracts prepared from *Escherichia coli*. Anal Biochem 232:98–106.

Berry A. 1996. Improving production of aromatic compounds in *Escherichia coli* by metabolic engineering. Trends Biotechnol 14:250–256.

Boiteux A, Markus M, Plesser T, Hess B, Malcovati M. 1983. Analysis of progress curves. Interaction of pyruvate kinase from *Escherichia coli* with fructose 1,6-bisphosphate and calcium ions. Biochem J 211:631–640.

Britton HG, Carreras J, Grisolia S. 1972. Mechanism of yeast phosphoglycerate mutase. Biochemistry 11:3008–3014.

Buziol S, Bashir I, Baumeister A, Claassen W, Rizzi M, Mailinger W, Reuss M. 2000. A new bioreactor coupled rapid stopped-flow-sampling-technique for measurement of transient metabolites in time windows of milliseconds. In: Proceedings of the Fourth International Congress on Biochemical Engineering. Stuttgart: Fraunhofer IRB. p 79–83.

Buziol S, Bashir I, Baumeister A, Claassen W, Noisommit-Rizzi N, Mailinger W, Reuss M. 2001. A new bioreactor coupled rapid stopped-flow sampling technique for measurements of metabolite dynamics on a subsecond time scale. Biotechnol Bioeng (in press).

Clark C, Holms WH. 1976. Control of the sequential utilisation of glucose and fructose by *Escherichia coli*. J Gen Microbiol 95:191–201.

Delgado J, Liao JC. 1995. Control of metabolic pathways by time-scale separation. Biosystems 36:55–70.

Deville-Bonne D, Laine R, Garel JR. 1991. Substrate antagonism in the kinetic mechanism of *Escherichia coli* phosphofructokinase-1. FEBS Lett 290:173–176.

Diaz Ricci JC. 1996. Influence of phosphoenolpyruvate on the dynamic behavior of phosphofructokinase of *Escherichia coli*. J Theor Biol 178:145–150.

Duggleby RG. 1994. Product inhibition of reversible enzyme-catalysed reactions. Biochim Biophys Acta 1209:238–240.

Dykhuizen DE, Hartl DL. 1983. Functional effects of PGI allozymes in *Escherichia coli*. Genetics 105:1–18.

Edwards JS, Palsson BO. 2000. Robustness analysis of the *Escherichia coli* metabolic network. Biotechnol Progr 16:927–939.

Ferenci T. 1996. Adaptation to life at micromolar nutrient levels: The regulation of *Escherichia coli* glucose transport by endoinduction and cAMP. FEMS Microbiol Rev 18:301–317.

Fifis T, Scopes RK. 1978. Purification of 3-phosphoglycerate kinase from diverse sources by affinity elution chromatography. Biochem J 175:311–319.

Flores N, Xiao J, Berry A, Bolivar F, Valle F. 1996. Pathway engineering for the production of aromatic compounds in *Escherichia coli*. Nat Biotechnol 14:620–623.

Galazzo JL, Bailey JE. 1990. Fermentation pathway kinetics and metabolic flux control in suspended and immobilized *Saccharomyces cerevisiae*. Enzyme Microb Technol 12:162–172.

Galazzo JL, Bailey JE. 1991. Errata. Enzyme Microb Technol 13:363.

Gosset G, Yong-Xiao J, Berry A. 1996. A direct comparison of approaches for increasing carbon flow to aromatic biosynthesis in *Escherichia coli*. J Indust Microbiol 17:47–52.

Grana X, Urena J, Ludevid D, Carreras J, Climent F. 1989. Purification, characterization and immunological properties of 2,3-bisphosphoglycerate-independent phosphoglycerate mutase from maize (Zea mays) seeds. Eur J Biochem 186:149–153.

Heiurich R, Schuster S. 1996. The regulation of cellular systems. Chapman & Hall, New York.

Hofmann E, Kopperschläger G. 1982. Phosphosfructokinase in yeast. In: Wood WA, editor. Methods in enzymology. New York: Academic Press. p 49–60.

Ingraham JL, Maaloe O, Neidhardt FC. 1983. Growth of the bacterial cell. Sunderland, MA: Sinauer Associates.

Johannes K-J, Hess B. 1973. Allosteric kinetics of pyruvate kinase of *Saccharomyces cerevisiae*. J Mol Biol 76:181–205.

Kaback HR. 1969. Regulation of sugar transport in isolated bacterial membrane preparations from *Escherichia coli*. Proc Natl Acad Sci USA 63:724–731.

Kameshita I, Tokushige M, Izui K, Katsuki H. 1979. Phosphoenolpyruvate carboxylase of *Escherichia coli*. Affinity labeling with bromopyruvate. J Biochem (Tokyo) 86:1251–1257.

Karp P, Riley M, Paley S, Pellegrini-Toole A, Krummenacker M. 1999. EcoCyc: Electronic encyclopedia of *E. coli* genes and metabolism. Nucl Acids Res 27:55.

Kotlarz D, Garreau H, Buc H. 1975. Regulation of the amount and of the activity of phosphofructokinase and pyruvate kinase in *Escherichia coli*. Biochim Biophys Acta 381:257–268.

Lavoinne A, Marchand JC, Chedeville A, Matray F. 1983. Kinetic studies of the reaction mechanism of rat liver phosphoglycerate kinase in the direction of ADP utilization. Biochimie 65:211–220.

Liao JC, Hou S, Chao Y. 1996. Pathway analysis, engineering and physiological considerations for redirecting central metabolism. Biotechnol Bioeng 52:129–140.

Liu J, Crawford JW, Viola R. 1996. The consequences of interactive noise for understanding the dynamics of complex biochemical systems. Dynam Stabil Syst 11:135–148.

Liu J, Crawford JW, Viola R, Goodman B. 1997. Prospects for advancing the understanding of complex biochemical systems. Plant Mol Biol 33:573–581.

Lowry OH, Passonneau JV. 1969. Phosphoglucomutase kinetics with the phosphates of fructose, glucose, mannose, ribose, and galactose. J Biol Chem 244:910–916.

Lu J, Liao JC. 1997. Metabolic engineering and control analysis for production of aromatics: role of transaldolase. Biotechnol Bioeng 53:132–138.

Mailinger W, Baumeister A, Reuss M, Rizzi M. 1998. Rapid and highly automated determination of adenine and pyridine nucleotides in extracts of *Saccharomyces cerevisiae* using a micro robotic sample preparation–HPLC system. J Biotechnol 63:155–166.

Mauch K, Vaseghi S, Reuss M. 2000. Quantitative analysis of metabolic and signaling pathways in *Saccharomyces cerevisiae*. In:

Schügerl K, Bellgardt KH, editors. Bioreaction engineering. Berlin: Springer. p 435–475.

Mauch K, Buziol S, Schmid J, Reuss M. 2001. Computer aided design of metabolic networks. AIChE Symp Series (in press).

Meyer S, Noisommit-Rizzi N, Reuss M, Neubauer P. 1999. Optimized analysis of intracellular adenosine and guanosine phosphates in *Escherichia coli*. Anal Biochem 271:43–52.

Molnar M, Vas M. 1993. Mg^{2+} affects the binding of ADP but not ATP to 3-phosphoglycerate kinase. Correlation between equilibrium dialysis binding and enzyme kinetic data. Biochem J 293:595–599.

Mulquiney PJ, Kuchel PW. 1999. Model of 2,3-bisphosphoglycerate metabolism in the human erythrocyte based on detailed enzyme kinetic equations: Equations and parameter refinement. Biochem J 342:581–596.

Neidhardt FC, Curtiss R III, Ingraham JL, Lin ECC, Low KB, Magasanik B, Reznikoff WS, Riley M, Schaechter M, Umbarger HE. 1996. *Escherichia coli* and *Salmonella*: cellular and molecular biology. Washington, DC: ASM Press.

Ni TC, Savageau MA. 1996. Model assement and refinement using strategies from biochemical systems theory: Application to metabolism in human red blood cells. J. Theor Biol 179:329–368.

Notley-McRobb L, Death A, Ferenci T. 1997. The relationship between external glucose concentration and cAMP levels inside *Escherichia coli*: Implications for models of phosphotransferase-mediated regulation of adenylate cyclase. Microbiology 143:1909–1918.

Orozco de Silva A. 1979. The 6-phosphogluconate dehydrogenase reaction in *Escherichia coli*. J Biol Chem 254:10237–10242.

Palsson B. 2000. The challenges of in silico biology. Nat Biotechnol 18:1147–1150.

Patnaik R, Liao JC. 1994. Engineering of *Escherichia coli* central metabolism for aromatic metabolite production with near theoretical yield. Appl Environ Microbiol 60:3903–3908.

Patnaik R, Spitzer RG, Liao JC. 1995. Pathway engineering for production of aromatics in *Escherichia coli*: Confirmation of stoichiometric analysis by independent modulation of aroG, tktA, and pps activities. Biotechnol Bioeng 46:361–370.

Pettersson G. 1990. What metabolite levels may be evolutionarily reached in the glycolytic pathway? Eur J Biochem 194:141–146.

Pramanik J, Keasling JD. 1997. Stoichiometric model of *Escherichia coli* metabolism: Incorporation of growth-rate dependent biomass composition and mechanistic energy requirements. Biotechnol Bioeng 56:398–421.

Pramanik J, Keasling JD. 1998. Effect of *Escherichia coli* biomass composition on central metabolic fluxes predicted by a stoichiometric model. Biotechnol Bioeng 60:230–238.

Preiss J, Greenberg E, Sabraw A. 1975. Biosynthesis of bacterial glycogen. Kinetic studies of a glucose-1-phosphate adenylyltransferase (EC 2.7.7.27) from a glycogen-deficient mutant of *Escherichia coli* B. J Biol Chem 250:7631–7638.

Richter O, Betz A, Giersch C. 1975. The response of oscillating glycolysis in the NADH/NAD system: A comparison between experiment and a computer model. Biosystems 7:137–146.

Rizzi M, Baltes M, Theobald U, Reuss M. 1997. In vivo analysis of metabolic dynamics in *Saccharomyces cerevisiae*: II. Mathematical model. Biotechnol Bioeng 55:592–608.

Sanwal BD. 1970. Regulatory mechanisms involving nicotinamide adenine nucleotides as allosteric effectors. III. Control of glucose 6-phosphate dehydrogenase. J Biol Chem 245:1626–1631.

Sauer U, Lasko DR, Fiaux J, Hochuli M, Glaser R, Szyperski T, Wüthrich K, Bailey JE. 1999. Metabolic flux ratio analysis of genetic and environmental modulations of *Escherichia coli* central carbon metabolism. J Bacteriol 181:6679–6687.

Schaefer U, Boos W, Takors R, Weuster-Botz D. 1999. Automated sampling device for monitoring intracellular metabolite dynamics. Anal Biochem 270:88–96.

Schauer M, Heinrich R, Rapoport SM. 1981. Mathematische Modellierung der Glykolyse und des Adeninnukleotidstoffwechsels menschlicher Erythrocyten. Acta Biol Med Germ 40:1659–1682.

Schmidt PP, Travers F, Barman T. 1995. Transient and equilibrium kinetic studies on yeast 3-phosphoglycerate kinase. Evidence that an intermediate containing 1,3-bisphosphoglycerate accumulates in the steady state. Biochemistry 34:824–832.

Schreyer R, Bock A. 1980. Phosphoglucose isomerase from *Escherichia coli* K10: Purification, properties and formation under aerobic and anaerobic condition. Arch Microbiol 127:289–298.

Schuster R, Holzhütter HG. 1995. Use of mathematical models for predicting the metabolic effect of large-scale enzyme activity alterations. Application to enzyme deficiencies of red blood cells. Eur J Biochem 229:403–418.

Spring TG, Wold F. 1971. The purification and characterization of *Escherichia coli* enolase. J Biol Chem 246:6797–6802.

Stephanopoulos GN, Simpson TW. 1997. Flux amplification in complex metabolic networks. Chem Eng Sci 52:2607–2627.

Stephanopoulos GN, Aristidou AA, Nielsen J. 1998. Metabolic engineering: Principles and methodologies. San Diego, CA: Academic Press.

Takama M, Nosoh Y. 1980. Purification and some properties of 6-phosphoglucose isomerase from *Bacillus caldotenax*. J Biochem 87:1821–1827.

Theobald U, Mailinger W, Reuss M, Rizzi M. 1993. *In vivo* Analysis of glucose-induced fast changes in yeast adenine nucleotide pool applying a rapid sampling technique. Anal Biochem 214:31–37.

Theobald U, Mailinger W, Baltes M, Rizzi M, Reuss M. 1997. In vivo analysis of metabolic dynamics in *Saccharomyces cerevisiae*: I. Experimental observations. Biotechnol Bioeng 55:305–316.

Torres JC, Guixe V, Babul J. 1997. A mutant phosphofructokinase produces a futile cycle during gluconeogenesis in *Escherichia coli*. Biochem J 327:675–684.

Varner JD. 2000. Large-scale prediction of phenotype: Concept Biotechnol Bioeng 69:664–678.

Vaseghi S, Baumeister A, Rizzi M, Reuss M. 1999. In vivo dynamics of the pentose phosphate pathway in *Saccharomyces cerevisiae*. Metab Eng 1:128–140.

Yi J, Nemeria N, McNally A, Jordan F, Machado RS, Guest JR. 1996. Effect of substitutions in the thiamin diphosphate-magnesium fold on the activation of the pyruvate dehydrogenase complex from *Escherichia coli* by cofactors and substrate. J Biol Chem 271:33192–33200.

Yoshinaga T. 1977. Structural specificity of the allosteric inhibitor of phosphoenolpyruvatecarboxylase of *Escherichia coli*. J Biochem (Tokyo) 81:665–671.